15
Colloids

INTRODUCTION

Dispersed Systems. It is important that the pharmacist understand the theory and technology of disperse systems. Although the quantitative aspects of this subject are not as well developed as are those of micromolecular chemistry, the theories that can be proposed in the field of colloidal chemistry are quite helpful in approaching the puzzling problems that arise in the preparation and dispensing of emulsions, suspensions, ointments, powders, and compressed dosage forms. A knowledge of interfacial phenomena and a familiarity with the characteristics of colloids and small particles are fundamental to an understanding of the behavior of pharmaceutical dispersions.

Dispersed systems consist of particulate matter, known as the *dispersed phase*, distributed throughout a *continuous*, or *dispersion*, *medium*. The dispersed material may range in size from particles of atomic and molecular dimensions to particles whose size is measured in millimeters. Accordingly, a convenient means of classifying dispersed systems is on the basis of the mean particle diameter of the dispersed material. Three size classifications are generally used, namely *molecular* dispersions, *colloidal* dispersions, and *coarse* dispersions. The size ranges assigned to these classes, together with some of the associated characteristics, are shown in Table 15–1. The size limits are somewhat arbitrary, there being no distinct transition between either molecular and colloidal dispersions or colloidal and coarse dispersions. For example, certain *macro-* (i.e., large) molecules, such as the polysaccharides, proteins, and polymers in general, are of sufficient size that they may be classified as forming both molecular and colloidal dispersions. Some suspensions and emulsions may contain a range of particle sizes such that the smaller particles lie within the colloidal range while the larger ones are classified as coarse particles.

Molecular dispersions are homogeneous in character and form true solutions. The properties of these systems have been discussed in the previous section of this text. Colloidal dispersions will be considered in the present chapter, powders and granules in Chapter 16, and coarse dispersions in Chapter 18; all are examples of heterogeneous systems.

Size and Shape of Colloidal Particles. Particles lying in the colloidal size range possess a surface area that is enormous compared with the surface area of an equal volume of larger particles. Thus, a cube having a 1-cm edge and a volume of 1 cm^3 has a total surface area of 6 cm^2. If the same cube is subdivided into smaller cubes, each having an edge of 100 μm, the total volume remains the same, but the total surface area increases to 600,000 cm^2. This represents a 10^5-fold increase in surface area. To compare quantitatively the surface areas of different materials, the term *specific surface* is used. This is defined as the surface area per unit weight or volume of material. In the example just given, the first sample had a specific surface of 6 cm^2/cm^3, while the second sample had a specific surface of 600,000 cm^2/cm^3. The possession of a large specific surface results in many of the unique properties of colloidal dispersions. For example, platinum is effective as a catalyst only when in the colloidal form as platinum black. This is because catalysts act by adsorbing the reactants onto their surface. Hence, their catalytic activity is related to their specific surface. The color of colloidal dispersions is related to the size of the particles present. Thus, as the particles in a red gold sol increase in size, the dispersion takes on a blue color. Antimony

TABLE 15–1 Classification of Dispersed Systems on the Basis of Particle Size*

Class	Range of Particle Size†	Characteristics of System	Examples
Molecular dispersion	Less than 1.0 nm (mμ)	Particles invisible in electron microscope; pass through ultrafilter and semipermeable membrane; undergo rapid diffusion.	Oxygen molecules, ordinary ions, glucose
Colloidal dispersion	1.0 nm to 0.5 μm	Particles not resolved by ordinary microscope although they may be detected under ultramicroscope; visible in electron microscope; pass through filter paper but do not pass semipermeable membrane; diffuse very slowly.	Colloidal silver sols, natural and synthetic polymers
Coarse dispersion	Greater than 0.5 μm (μ)	Particles visible under microscope; do not pass through normal filter paper or dialyze through semipermeable membrane; particles do not diffuse.	Grains of sand, most pharmaceutical emulsions and suspensions, red blood cells

*Modified from Oswald: Kuhn's Kolloid chemisches Taschenbuch, as quoted in part from H. B. Weiser, *Colloid Chemistry*, 2nd Edition, Wiley, New York, 1949.
†A micrometer (μm), formerly called a micron (μ), is a unit of length equal to one thousandth of a millimeter or 10^{-3} mm. A nanometer (nm), formerly called a millimicron (mμ), is one thousandth of a micron or 10^{-6} mm. It follows that 1 cm is equal to 10^4 μm or 10^7 nm.

and arsenic trisulfides change from red to yellow as the particle size is reduced from that of a coarse powder to that within the colloidal size range.

Because of their size, colloidal particles may be separated from molecular particles with relative ease. The technique of separation, known as *dialysis*, uses a semipermeable membrane of collodion or cellophane, the pore size of which will prevent the passage of colloidal particles, yet will permit small molecules and ions, such as urea, glucose, and sodium chloride, to pass through. The principle is illustrated in Figure 15–1, which shows that, at equilibrium, the colloidal material is retained in compartment A, while the subcolloidal material is distributed equally on both sides of the membrane. By continually removing the liquid in compartment B, it is possible to obtain colloidal material in A that is free from subcolloidal contaminants.

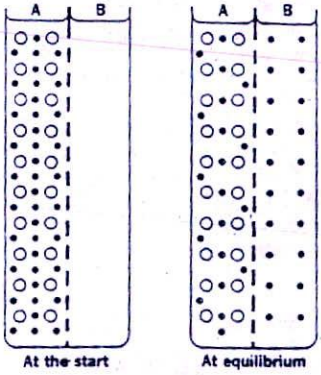

Fig. 15–1. Sketch showing the removal of electrolytes from colloidal material by diffusion through a semipermeable membrane. Conditions on the two sides, A and B, of the membrane are shown at the start and at equilibrium. The open circles are the colloidal particles that are too large to pass through the membrane. The solid dots are the electrolyte particles that pass through the pores of the membrane.

Dialysis may also be used to obtain subcolloidal material that is free from colloidal contamination—in this case, one simply collects the effluent. *Ultrafiltration* has also been used to separate and purify colloidal material. According to one variation of the method, filtration is conducted under negative pressure (suction) through a dialysis membrane supported in a Büchner funnel. When dialysis and ultrafiltration are used to remove charged impurities, such as ionic contaminants, the process may be hastened by the use of an electric potential across the membrane. This process is called *electrodialysis*.

Dialysis has been used increasingly in recent years to study the binding of materials of pharmaceutical significance to colloidal particles. Dialysis occurs in vivo. Thus, ions and small molecules pass readily from the blood, through a natural semipermeable membrane, to the tissue fluids; the colloidal components of the blood remain within the capillary system. The principle of dialysis is utilized in the artificial kidney, which removes small-molecular-weight impurities from the body by passage through a semipermeable membrane.

The shape adopted by colloidal particles in dispersion is important, since the more extended the particle, the greater its specific surface and the greater the opportunity for attractive forces to develop between the particles of the dispersed phase and the dispersion medium. A colloidal particle is something like a hedgehog—in a friendly environment, it unrolls and exposes maximum surface area. Under adverse conditions, it rolls up and reduces its exposed area. Some representative shapes of spherocolloids and fibrous colloids are shown in Figure 15–2. As will be seen in later discussions, such properties as flow, sedimentation, and osmotic pressure are affected by changes in the shape of colloidal particles. Particle shape may also influence pharmacologic action. Cromoglycic acid, an agent administered by inhalation to control asthmatic attacks, was found by Chan and Gonda[1] to be suitably deposited

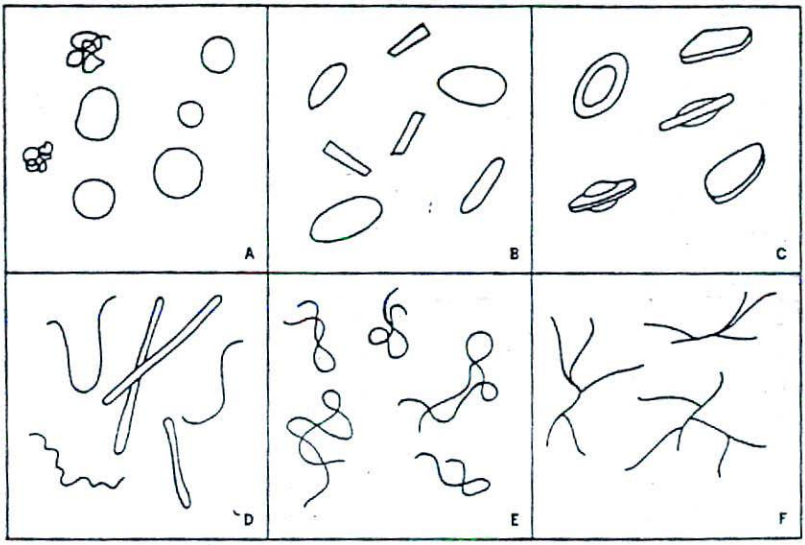

Fig. 15–2. Some shapes that may be assumed by colloidal particles: *(a)* spheres and globules; *(b)* short rods and prolate ellipsoids; *(c)* oblate ellipsoids and flakes; *(d)* long rods and threads; *(e)* loosely coiled threads; *(f)* branched threads.

in the respiratory tract when prepared as well-formed rod-shaped crystals.

Pharmaceutical Applications of Colloids. Certain medicinals have been found to possess unusual or increased therapeutic properties when formulated in the colloidal state. Colloidal silver chloride, silver iodide, and silver protein are effective germicides and do not cause the irritation that is characteristic of ionic silver salts. Coarsely powdered sulfur is poorly absorbed when administered orally, yet the same dose of colloidal sulfur may be absorbed so completely as to cause a toxic reaction and even death. Colloidal copper has been used in the treatment of cancer, colloidal gold as a diagnostic agent for paresis, and colloidal mercury for syphilis.

Many natural and synthetic polymers are important in contemporary pharmaceutical practice. Polymers are macromolecules formed by the polymerization or condensation of smaller, noncolloidal, molecules. Proteins are important natural colloids and are found in the body as components of muscle, bone, and skin. The plasma proteins are responsible for binding certain drug molecules to such an extent that the pharmacologic activity of the drug is affected. Naturally occurring plant macromolecules such as starch and cellulose that are used as pharmaceutical adjuncts are capable of existing in the colloidal state. Hydroxyethyl starch (HES) is a macromolecule used as a plasma substitute. Other synthetic polymers are applied as coatings to solid dosage forms to protect drugs that are susceptible to atmospheric moisture or degradation under the acid conditions of the stomach. Colloidal electrolytes (surface-active agents) are sometimes used to increase the solubility, stability, and taste of certain compounds in aqueous and oily pharmaceutical preparations.

TYPES OF COLLOIDAL SYSTEMS

Colloidal systems are best classified into three groups—lyophilic, lyophobic, and association—on the basis of the interaction of the particles, molecules, or ions of the dispersed phase with the molecules of the dispersion medium.

Lyophilic Colloids. Systems containing colloidal particles that interact to an appreciable extent with the dispersion medium are referred to as *lyophilic* (solvent-loving) colloids. Owing to their affinity for the dispersion medium, such materials form colloidal dispersions, or *sols*, with relative ease. Thus, lyophilic colloidal sols are usually obtained simply by dissolving the material in the solvent being used. For example, the dissolution of acacia or gelatin in water or celluloid in amyl acetate leads to the formation of a sol.

The various properties of this class of colloids are due to the attraction between the dispersed phase and the dispersion medium, which leads to *solvation*, the attachment of solvent molecules to the miecules of the dispersed phase. In the case of hydrophilic colloids, in which water is the dispersion medium, that is termed *hydration*. Most lyophilic colloids are organic molecules, for example, gelatin, acacia, insulin, albumin, rubber, and polystyrene. Of these, the first four produce lyophilic colloids in aqueous dispersion media (hydrophilic sols). Rubber and polystyrene form lyo-

philic colloids in nonaqueous, organic, solvents. These materials accordingly are referred to as *lipophilic* colloids. These examples illustrate the important point that the term *lyophilic* has meaning only when applied to the material dispersed in a specific dispersion medium. A material that forms a lyophilic colloidal system in one liquid (e.g., water) may not do so in another liquid (e.g., benzene).

Lyophobic Colloids. The second class of colloids is composed of materials that have little attraction, if any, for the dispersion medium. These are the *lyophobic* (solvent-hating) colloids and, predictably, their properties differ from those of the lyophilic colloids. This is due primarily to the absence of a solvent sheath around the particle. Lyophobic colloids are generally composed of inorganic particles dispersed in water. Examples of such materials are gold, silver, sulfur, arsenous sulfide, and silver iodide.

In contrast to lyophilic colloids, it is necessary to use special methods to prepare lyophobic colloids. These are (*a*) dispersion methods, in which coarse particles are reduced in size, and (*b*) condensation methods, in which materials of subcolloidal dimensions are caused to aggregate into particles within the colloidal size range. Dispersion may be achieved by the use of high-intensity ultrasonic generators operating at frequencies in excess of 20,000 cycles per second. A second dispersion method involves the production of an electric arc within a liquid. Owing to the intense heat generated by the arc, some of the metal of the electrodes is dispersed as vapor, which condenses to form colloidal particles. Milling and grinding processes may be used, although their efficiency is low. So-called colloid mills, in which the material is sheared between two rapidly rotating plates set close together, reduce only a small amount of the total particles to the colloidal size range.

The required conditions for the formation of lyophobic colloids by condensation or aggregation involve a high degree of initial supersaturation followed by the formation and growth of nuclei. Supersaturation may be brought about by change in solvent or reduction in temperature. For example, if sulfur is dissolved in alcohol and the concentrated solution is then poured into an excess of water, many small nuclei form in the supersaturated solution. These grow rapidly to form a colloidal sol. Other condensation methods depend on a chemical reaction, such as reduction, oxidation, hydrolysis, or double decomposition. Thus, neutral or slightly alkaline solutions of the noble metal salts, when treated with a reducing agent such as formaldehyde or pyrogallol, form atoms that combine to form charged aggregates. The oxidation of hydrogen sulfide leads to the formation of sulfur atoms and the production of a sulfur sol. If a solution of ferric chloride is added to a large volume of water, hydrolysis occurs with the formation of a red sol of hydrated ferric oxide. Chromium and aluminum salts also hydrolyze in this manner. Finally, the double decomposition between hydrogen sulfide and arsenous acid results in an arsenous sulfide sol. If an excess of hydrogen sulfide is used, HS^- ions are adsorbed onto the particles. This creates a large negative charge on the particles, leading to the formation of a stable sol.

Association Colloids: Micelles and the CMC. *Association, or amphiphilic*, colloids form the third group in this classification. As we have seen in Chapter 14, which dealt with interfacial phenomena (p. 370), certain molecules or ions, termed *amphiphiles* or *surface-active agents*, are characterized by having two distinct regions of opposing solution affinities within the same molecule or ion. When present in a liquid medium at low concentrations, the amphiphiles exist separately and are of such a size as to be subcolloidal. As the concentration is increased, aggregation occurs over a narrow concentration range. These aggregates, which may contain 50 or more monomers, are called *micelles*. Since the diameter of each micelle is of the order of 50 Å, micelles lie within the size range we have designated as colloidal. The concentration of monomer at which micelles form is termed the *critical micelle concentration*, or *cmc*. The number of monomers that aggregate to form a micelle is known as the *aggregation number* of the micelle.

The phenomenon of micelle formation can be explained as follows. Below the cmc, the concentration of amphiphile undergoing adsorption at the air–water interface increases as the total concentration of amphiphile is raised. Eventually a point is reached at which both the interface and the bulk phase become saturated with monomers. This is the cmc. Any further amphiphile added in excess of this concentration aggregates to form micelles in the bulk phase and, in this manner, the free energy of the system is reduced. The effect of micellization on some of the physical properties of solutions containing surface-active agents is shown in Figure 15–3. Note particularly that surface tension decreases up to the cmc. From Gibbs' adsorption equation (p. 370), this means increasing interfacial adsorption. Above the cmc, the surface tension remains essentially constant, showing that the interface is saturated and micelle formation has taken place in the bulk phase.

In the case of amphiphiles in water, the hydrocarbon chains face inward into the micelle to form, in effect, their own hydrocarbon environment. Surrounding this hydrocarbon core are the polar portions of the amphiphiles associated with the water molecules of the continuous phase. Aggregation also occurs in nonpolar liquids. The orientation of the molecules is now reversed, however, with the polar heads facing inward while the hydrocarbon chains are associated with the continuous nonpolar phase. These situations are shown in Figure 15–4, which also shows some of the shapes postulated for micelles. It seems likely that spherical micelles exist at concentrations relatively close to the cmc. At higher concentrations, laminar micelles have an increasing tendency to form and exist in equilibrium with sperical micelles. The student is cautioned against

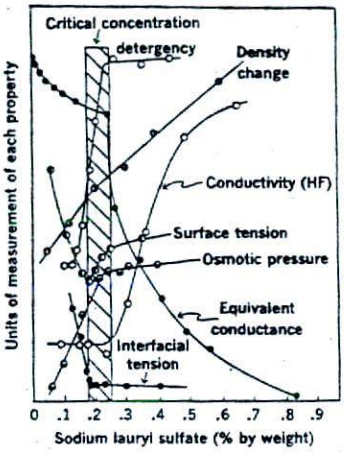

Fig. 15–3. Properties of surface-active agents showing changes that occur sharply at the critical micelle concentration. (Modified from Preston, W. J. Phys. Coll. Chem. 52, 85, 1948. Copyright © 1948, The Williams & Wilkins Co., Baltimore.)

regarding micelles as solid particles. The individual molecules forming the micelle are in dynamic equilibrium with those monomers in the bulk and at the interface.

As with lyophilic sols, formation of association colloids is spontaneous, provided that the concentration of the amphiphile in solution exceeds the cmc.

Amphiphiles may be anionic, cationic, nonionic, or ampholytic (zwitterionic), and this provides a convenient means of classifying association colloids. A typical example of each type is given in Table 15–2. Thus, Figure 15–4*a* represents the micelle of an anionic association colloid. A certain number of the sodium ions are attracted to the surface of the micelle, reducing the overall negative charge somewhat. These bound ions are termed *gegenions*.

Mixtures of two or more amphiphiles are usual in pharmaceutical formulations. Assuming an ideal mixture, the cmc of the mixture can be predicted from the cmc values of the pure amphiphiles and their mole fractions x in the mixture, according to the expresssion[2]

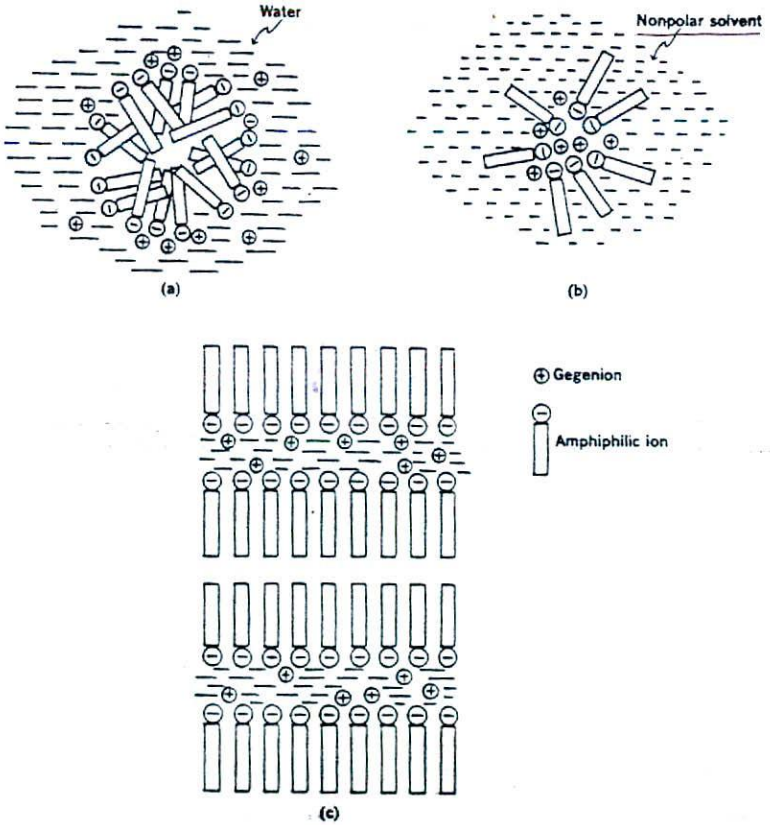

Fig. 15–4. Some probable shapes of micelles: *(a)* spherical micelle in aqueous media; *(b)* reversed micelle in nonaqueous media; *(c)* laminar micelle, formed at higher amphiphile concentration, in aqueous media.

TABLE 15–2. *Classification of Association Colloids*

Type	Compound	Amphiphile	Gegenions
Anionic	Sodium lauryl sulfate	$CH_3(CH_2)_{11}OSO_3^-$	Na^+
Cationic	Cetyl trimethylammonium bromide	$CH_3(CH_2)_{15}N^+(CH_3)_3$	Br^-
Nonionic	Polyoxyethylene lauryl ether	$CH_3(CH_2)_{10}CH_2O(CH_2OCH_2)_{23}H$	—
Ampholytic	Dimethyldodecylammonio-propane sulfonate	$CH_3(CH_2)_{11}N^+(CH_3)_2(CH_2)_3OSO_2^-$	—

TABLE 15–3. *Comparison of Properties of Colloidal Sols**

Lyophilic	Association (Amphiphilic)	Lyophobic
Dispersed phase consists generally of large organic *molecules* lying within colloidal size range.	Dispersed phase consists of aggregates *(micelles)* of small organic molecules or ions whose size *individually* is below the colloidal range.	Dispersed phase ordinarily consists of inorganic particles, such as gold or silver.
Molecules of the dispersed phase are solvated, i.e., they are associated with the molecules comprising the dispersion medium.	Hydrophilic or lipophilic portion of the molecule is solvated, depending on whether the dispersion medium is aqueous or nonaqueous.	Little, if any, interaction (solvation) occurs between particles and dispersion medium.
Molecules disperse spontaneously to form colloidal solution.	Colloidal aggregates are formed spontaneously when the concentration of amphiphile exceeds the critical micelle concentration (cmc).	Material does not disperse spontaneously, and special procedures therefore must be adopted to produce colloidal dispersion.
Viscosity of the dispersion medium ordinarily is increased greatly by the presence of the dispersed phase. At sufficiently high concentrations, the sol may become a gel. Viscosity and gel formation are related to solvation effects and to the shape of the molecules, which are usually highly asymmetric.	Viscosity of the system increases as the concentration of the amphiphile increases, as micelles increase in number and become asymmetric.	Viscosity of the dispersion medium is not greatly increased by the presence of lyophobic colloidal particles, which tend to be unsolvated and symmetric.
Dispersions are stable generally in the presence of electrolytes. They may be salted out by high concentrations of very soluble electrolytes. Effect is due primarily to desolvation of lyophilic molecules.	In aqueous solutions, the critical micelle concentration is reduced by the addition of electrolytes. Salting-out may occur at higher salt concentrations.	Lyophobic dispersions are unstable in the presence of even small concentrations of electrolytes. Effect is due to neutralization of the charge on the particles. Lyophilic colloids exert a protective effect.

*From J. Swarbrick and A. Martin, *American Pharmacy*, 6th Edition, Lippincott, Philadelphia, 1966, p. 161.

$$\frac{1}{\text{cmc}} = \frac{x_1}{\text{cmc}_1} + \frac{x_2}{\text{cmc}_2} \qquad (15-1)$$

Example 15–1. Compute the cmc of a mixture of *n*-dodecyl octaoxyethylene glycol monoether ($C_{12}E_8$) and *n*-dodecyl β-D-maltoside (DM). The cmc of $C_{12}E_8$ is $\text{cmc}_1 = 8.1 \times 10^{-5}$ mole/liter and its mole fraction is $x_1 = 0.75$; the cmc of DM is $\text{cmc}_2 = 15 \times 10^{-5}$ mole/liter.

$$x_2 = (1 - x_1) = (1 - 0.75) = 0.25$$

From equation (15–1),

$$\frac{1}{\text{cmc}} = \frac{0.75}{8.1 \times 10^{-5}} + \frac{(1 - 0.75)}{15 \times 10^{-5}} = 10926$$

$$\text{cmc} = \frac{1}{10926} = 9.15 \times 10^{-5} \text{ mole/liter}$$

The experimental value is 9.3×10^{-5} mole/liter.

The properties of lyophilic, lyophobic, and association colloids are outlined in Table 15–3. These properties, together with the relevant methods, will be discussed in the following sections.

OPTICAL PROPERTIES OF COLLOIDS

The Faraday–Tyndall Effect. When a strong beam of light is passed through a colloidal sol, a visible cone, resulting from the scattering of light by the colloidal particles, is formed. This is the *Faraday–Tyndall effect.*

The *ultramicroscope*, developed by Zsigmondy, allows one to examine the light points responsible for the *Tyndall cone*. An intense light beam is passed through the sol against a dark background at right angles to the plane of observation, and, although the particles cannot be seen directly, the bright spots corresponding to particles can be observed and counted.

Electron Microscope. The use of the ultramicroscope has declined in recent years since it frequently does not resolve lyophilic colloids. The *electron microscope*, capable of yielding pictures of the actual particles, even those approaching molecular dimensions, is now widely used to observe the size, shape, and structure of colloidal particles.

The success of the electron microscope is due to its high resolving power, which may be defined in terms of d, the smallest distance by which two objects are separated and yet remain distinguishable. The smaller the wavelength of the radiation used, the smaller is d and the greater the resolving power. The optical microscope uses visible light as its radiation source and is only able to resolve two particles separated by about 200 Å. The radiation source of the electron microscope is a beam of high-energy electrons having wavelengths in the region of 0.1 Å. With current instrumentation, this results in d being approximately 5 Å, a much increased power of resolution over the optical microscope.

Light Scattering. This property depends on the Faraday–Tyndall effect and is a widely used method for determining the molecular weight of colloids. It may also be used to obtain information as to the shape and size of these particles. Scattering may be described in terms of the turbidity, τ, the fractional decrease in intensity due to scattering as the incident light passes through 1 cm of solution. It may be expressed as the intensity of light scattered in all directions, I_s, divided by the intensity of the incident light, I. At a given concentration of dispersed phase, the turbidity is proportional to the molecular weight of the lyophilic colloid. Because of the low turbidities of most lyophilic colloids, it is more convenient to measure the scattered light (at a particular angle relative to the incident beam) rather than the transmitted light.

The turbidity can then be calculated from the intensity of the scattered light provided that the dimensions of the particle are small compared with the wavelength of the light used. The molecular weight of the colloid may be obtained from the following equation:

$$Hc/\tau = 1/M + 2Bc \qquad (15\text{–}2)$$

in which τ is the turbidity in cm^{-1}, c the concentration of solute in g/cm^3 of solution, M the weight average molecular weight in g/mole or daltons, and B an interaction constant (see osmotic pressure, pp. 401–402). H is constant for a particular system and is written

$$H = \frac{32\pi^3 n^2 (dn/dc)^2}{3\lambda^4 N}$$

in which n (dimensionless) is the refractive index of the solution of concentration c (g/cm^3) at a wavelength λ in cm^{-1}, (dn/dc) is the change in refractive index with concentration at c, and N is Avogadro's number. A plot of Hc/τ against concentration, Figure 15–5, results in a straight line with a slope of $2B$. The intercept on the Hc/τ axis is $1/M$, the reciprocal of which yields the molecular weight of the colloid (see Problem 15–2).

When the molecule is asymmetric, the intensity of the scattered light varies with the angle of observation. Data of this kind permit an estimation of the shape and size of the particles. Light scattering has been used to study proteins, synthetic polymers, association colloids, and lyophobic sols.

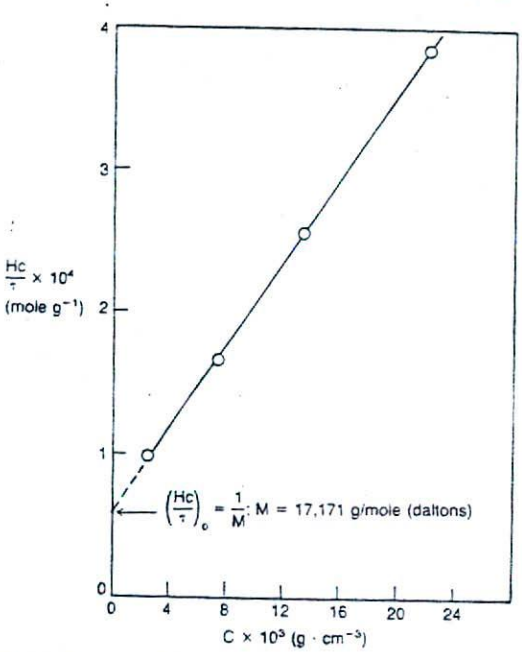

Fig. 15–5. A plot of Hc/τ against the concentration of a polymer (colloid) (see Problem 15–2).

Chang and Cardinal[3] used light scattering to study the pattern of self-association in aqueous solution of the bile salts sodium deoxycholate and sodium taurodeoxycholate. Analysis of the data showed that the bile salts associate to form dimers, trimers, and tetramers, and a larger aggregate of variable size.

Racey et al.[4] used quasi-elastic light scattering (QELS), a new light-scattering technique that uses laser light and may determine diffusion coefficients and particle sizes (Stokes' diameter, p. 425) of macromolecules in solution. Quasi-elastic light scattering allowed the examination of heparin aggregates in commercial preparations stored for various times and at various temperatures. Both storage time and refrigeration caused an increase in the aggregation state of heparin solutions. It has not yet been determined whether the change in aggregation has any effect on the biologic activity of commercial preparations.

Light Scattering and Micelle Molecular Weight. Equation (15–2) can be applied after suitable modification to compute the molecular weight of colloidal aggregates and micelles. When amphiphilic molecules associate to form micelles, the turbidity of the micellar dispersion differs from the turbidity of the solution of the amphiphilic molecules because micelles are now also present in equilibrium with the monomeric species. Below the cmc, the concentration of monomers in-

creases linearly with the total concentration, c; above the cmc the monomer concentration remains nearly constant; that is, $c_{monomer} \cong$ cmc. The concentration of micelles may therefore be written

$$c_{micelle} = c - c_{monomer} = c - c_{cmc} \qquad (15-3)$$

The corresponding turbidity of the solution due to the presence of micelles is obtained by subtracting the turbidity due to monomers, $\tau_{monomer} = \tau_{cmc}$, from the total turbidity of the solution:

$$\tau_{mic.} = \tau - \tau_{cmc} \qquad (15-4)$$

Accordingly, equation (15–2) is modified to

$$\frac{H(c - c_{cmc})}{(\tau - \tau_{cmc})} = \frac{1}{M} + 2B(c - c_{cmc}) \qquad (15-5)$$

where the subscript cmc stands for turbidity or concentration at the critical micelle concentration, and B and H have the same meaning as in equation (15–2). Thus, the molecular weight M of the micelle and the second virial coefficient B (p. 401) are obtained from the intercept and the slope, respectively, of a plot of $H(c - c_{cmc})/(\tau - \tau_{cmc})$ versus $(c - c_{cmc})$. Equation (15–5) is valid for two-component systems, that is, for a micelle and a molecular surfactant in this instance.

When the micelles interact neither among themselves nor with the molecules of the medium, the slope of a plot of equation (15–5) is zero; that is, the second virial coefficient B is zero and the line is parallel to the horizontal axis, as seen in Figure 15–6. This behavior is typical of nonionic and zwitterionic micellar systems in which the size distribution is narrow. However, as the concentration of micelles increases, intermicellar interactions lead to positive values of B, the slope of the line having a positive value. For ionic micelles the plots are linear with positive slopes, owing to repulsive intermicellar interactions that result in positive values of the interaction coefficient, B. A negative second virial coefficient is usually an indication that the micellar system is polydisperse.[5,6]

Example 15–2. Using the following data compute the molecular weight of micelles of dimethylalkylammoniopropane sulfonate, a zwitterionic surfactant investigated by Herrmann[6]:

$(c - c_{cmc}) \times 10^3$ (g/mL)	0.98	1.98	2.98	3.98	4.98
$\left[\frac{H(c - c_{cmc})}{\tau - \tau_{cmc}}\right] \times 10^5$ (mole/g)	1.66	1.65	1.66	1.69	1.65

Using equation (15–5), the micellar molecular weight is obtained from a plot of $\frac{H(c - c_{cmc})}{\tau - \tau_{cmc}}$ versus $(c - c_{cmc})$ (see Fig. 15–6); the intercept is $\frac{1}{M} = 1.66 \times 10^{-5}$ mole/g; therefore, $M = 60{,}241$ g/mole. The slope is zero; that is, $2B$ in equation (15–5) is zero.

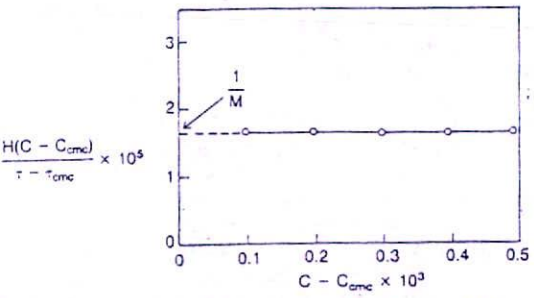

Fig. 15–6. A plot of $H(c - c_{cmc})/\tau - \tau_{cmc}$ versus $(c - c_{cmc}) \times 10^3$ for a zwitterionic surfactant in which B is zero.[6]

KINETIC PROPERTIES OF COLLOIDS

Grouped under this heading are several properties of colloidal systems that relate to the motion of particles with respect to the dispersion medium. The motion may be thermally induced (Brownian movement, diffusion, osmosis), gravitationally induced (sedimentation), or applied externally (viscosity). Electrically induced motion is considered in the section on electric properties of colloids.

Brownian Motion. Long before Zsigmondy had described the random movement of colloidal particles in the microscopic field, Robert Brown (1827) studied this phenomenon. The erratic motion, which may be observed with particles as large as about 5 μm, was later explained as resulting from the bombardment of the particles by the molecules of the dispersion medium. The motion of the molecules cannot be observed, of course, since the molecules are too small to see. The velocity of the particles increases with decreasing particle size. Increasing the viscosity of the medium, which may be accomplished by the addition of glycerin or a similar agent, decreases and finally stops the Brownian movement.

Diffusion. Particles diffuse spontaneously from a region of higher concentration to one of lower concentration until the concentration of the system is uniform throughout. Diffusion is a direct result of Brownian movement.

According to *Fick's first law* (p. 325), the amount dq of substance diffusing in time dt across a plane of area S is directly proportional to the change of concentration dc with distance traveled dx.

Fick's law is written

$$dq = -DS\frac{dc}{dx}dt \qquad (15-6)$$

D is the *diffusion coefficient*, the amount of material diffusing per unit time across a unit area when dc/dx, called the *concentration gradient*, is unity. D thus has the dimensions of area per unit time. The coefficient may be obtained in colloidal chemistry by diffusion experiments in which the material is allowed to pass through a porous disc, and samples are removed and

analyzed periodically. Another method involves measuring the change in the concentration or refractive index gradient of the free boundary that is formed when the solvent and colloidal solution are brought together and allowed to diffuse.

If the colloidal particles can be assumed to be approximately spherical, the following equation, suggested by Sutherland and Einstein, can be used to obtain the radius of the particle and the particle weight or molecular weight:

$$D = \frac{kT}{6\pi\eta r}$$

or

$$D = \frac{RT}{6\pi\eta r N} \qquad (15-7)$$

in which D is the diffusion coefficient obtained from Fick's law as already explained, k is the Boltzmann constant, R is the molar gas constant, T is the absolute temperature, η is the viscosity of the solvent, r is the radius of the spherical particle, and N is Avogadro's number. Equation (15–7) is called the *Sutherland–Einstein* or the *Stokes–Einstein* equation. The measured diffusion coefficient may be used to obtain the molecular weight of approximately spherical molecules, such as egg albumin and hemoglobin, by use of the equation,

$$D = \frac{RT}{6\pi\eta N}\sqrt[3]{\frac{4\pi N}{3M\bar{v}}} \qquad (15-8)$$

in which M is molecular weight and $\bar{v}$ is the partial specific volume (approximately equal to the volume in cm^3 of 1 gram of the solute, obtained from density mesurements).

Example 15–3. The diffusion coefficient for a spherical protein at 20° C is 7.0×10^{-7} cm^2/sec and the partial specific volume is 0.75 cm^3/g. The viscosity of the solvent is 0.01 poise (0.01 g/cm sec). Compute (*a*) the molecular weight and (*b*) the radius of the protein particle.

(*a*) By rearranging equation (15–8), we obtain

$$M = \frac{1}{162\bar{v}^3}\left(\frac{1}{\pi N}\right)^2\left(\frac{RT}{D\eta}\right)^3$$

$$M = \frac{1}{162 \times 0.75}\left(\frac{1}{3.14 \times (6.02 \times 10^{23})}\right)^2 \cdot \left(\frac{(8.31 \times 10^7) \times 293}{(7.0 \times 10^{-7}) \times 0.01}\right)^3$$

$\approx 100{,}000$ g/mole

(*b*) From equation (15–7):

$$r = \frac{RT}{6\pi\eta N D}$$

$$= \frac{(8.31 \times 10^7) \times 293}{6 \times 3.14 \times 0.01 \times (6.02 \times 10^{23}) \times (7.0 \times 10^{-7})}$$

$= 31 \times 10^{-8}$ cm = 31 Å

Osmotic Pressure. The van't Hoff equation

$$\pi = cRT \qquad (15-9)$$

can be used to calculate the molecular weight of a colloid in a dilute solution. Replacing c with c_g/M in equation (15–9), in which c_g is the grams of solute per liter of solution and M is the molecular weight, we obtain

$$\pi = \frac{c_g}{M}RT \qquad (15-10)$$

Then,

$$\frac{\pi}{c_g} = \frac{RT}{M} \qquad (15-11)$$

which applies in a very dilute solution. The quantity π/c_g for a polymer having a molecular weight of, say, 50,000 is often a linear function of the concentration c_g, and the following equation can be written:

$$\frac{\pi}{c_g} = RT\left(\frac{1}{M} + Bc_g\right) \qquad (15-12)$$

in which B is a constant for any particular solvent/solute system and depends on the degree of interaction between the solvent and the solute molecules. The term Bc_g in equation (15–12) is needed because equation (15–11) holds only for ideal solutions, namely, those containing low concentrations of spherocolloids. With linear lyophilic molecules, deviations occur because the solute molecules become solvated, leading to a reduction in the concentration of "free" solvent and an apparent increase in solute concentration. The role of B in estimating the asymmetry of particles and their interactions with solute has been discussed by Hiemenz.[7]

A plot of π/c_g against c_g generally results in one of three lines (Fig. 15–7), depending on whether the system is ideal (line I) or real (lines II and III). Equation (15–11) applies to line I, and equation (15–12)

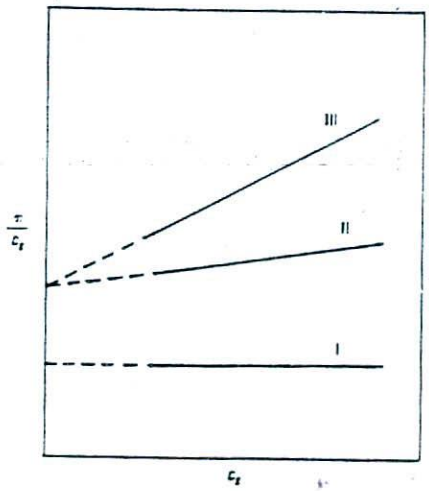

Fig. 15–7. Determination of molecular weight by means of the osmotic pressure method. Extrapolation of the line to the vertical axis where $c_g = 0$ gives RT/M, from which M is obtained. Refer to text for significance of lines I, II, and III. Lines II and III are taken to represent two samples of a species of hemoglobin.

describes lines II and III. The intercept is RT/M, and if the temperature at which the determination was carried out is known, the molecular weight of the solute can be calculated. In lines II and III, the slope of the line is B, the interaction constant. In line I, B equals zero and is typical of a dilute spherocolloidal system. Line III is typical of a linear colloid in a solvent having a high affinity for the dispersed particles. Such a solvent is referred to as a "good" solvent for that particular colloid. There is a marked deviation from ideality as the concentration is increased and B is large. At higher concentrations, or where interaction is marked, type III lines can become nonlinear, requiring that equation (15–12) be expanded and written as a power series:

$$\frac{\pi}{c_g} = RT\left(\frac{1}{M} + Bc_g + Cc_2 + \cdots\right) \qquad (15-13)$$

in which C is another interaction constant. Line II depicts the situation in which the same colloid is present in a relatively poor solvent having a reduced affinity for the dispersed material. Note, however, that the extrapolated intercept on the π/c_g axis is identical for both lines II and III, showing that the calculated molecular weight is independent of the solvent used.

Example 15–4. Let us assume that the intercept $(\pi/c_g)_o$ for line III in Figure 15–7 has the value 3.623×10^{-4} liter atm/gram, and the slope of the line is 1.80×10^{-6} liter^2 atm g^{-2}. What is the molecular weight and the second virial coefficient B for a sample of hemoglobin in the data given here?

In Figure 15–7, line III crosses the vertical intercept at the same point as line II. These two samples of hemoglobin have the same *limiting reduced osmotic pressure*, as $(\pi/c_g)_o$ is called, and therefore have the same molecular weight. The B values, and therefore the shape of the two samples and their interaction with the medium, differ as evidenced by the different slopes of lines II and III.

At the intercept $(\pi/c_g)_o = RT/M$. Therefore,

$$M = RT/(\pi/c_g)_o = \frac{0.08206 \text{ liter atm/deg mole})(298^\circ \text{ K})}{3.623 \times 10^{-4} \text{ liter atm g}^{-1}}$$

$M = 67{,}496$ g/mole (daltons) for both hemoglobins.

The slope of line III, representing one of the hemoglobin samples, is divided by RT to obtain B, as observed in equation (15–12):

$$B = 1.80 \times 10^{-6} \text{ liter}^2 \text{ atm g}^{-2}/(0.08206 \text{ liter atm/mole deg})(298^\circ \text{ K})$$
$$= 7.36 \times 10^{-8} \text{ liter mole g}^{-2}$$

The other hemoglobin sample, represented by line II, has a slope of 4.75×10^{-9} liter^2 atm g^{-2}, and its B value is therefore calculated as follows:

$$B = 4.75 \times 10^{-9} \text{ liter}^2 \text{ atm g}^{-2}/(0.08206 \text{ liter atm/mole deg})(298^\circ \text{ K})$$
$$= 1.94 \times 10^{-10} \text{ liter mole g}^{-2}$$

What would you estimate the B value to be for the protein represented by line I? Would you assume its molecular weight to be larger or smaller than that of samples II and III? Referring to equations (15–11) and (15–12) will assist you in arriving at your answers.

Sedimentation. The velocity v of sedimentation of spherical particles having a density ρ in a medium of density ρ_0 and a viscosity η_0 is given by *Stokes' law:*

$$v = \frac{2r^2(\rho - \rho_o)g}{9\eta_o} \qquad (15-14)$$

in which g is the acceleration due to gravity. If the particles are subjected only to the force of gravity, then the lower size limit of particles obeying Stokes' equation is about 0.5 μm. This is because Brownian movement becomes significant and tends to offset sedimentation due to gravity and promotes mixing instead. Consequently, a stronger force must be applied to bring about the sedimentation of colloidal particles in a quantitative and measurable manner. This is accomplished by use of the *ultracentrifuge*, developed by Svedberg in 1925, which can produce a force a million times that of gravity.

In a centrifuge, the acceleration of gravity is replaced by $\omega^2 x$, in which ω is the angular velocity and x is the distance of the particle from the center of rotation. Equation (15–14) is accordingly modified to

$$v = \frac{dx}{dt} = \frac{2r^2(\rho - \rho_o)\omega^2 x}{9\eta_o}$$

The speed at which a centrifuge is operated is commonly expressed in terms of the number of revolutions per minute (rpm) of the rotor. It is frequently more desirable to express the rpm as angular acceleration ($\omega^2 x$) or the number of times that the force of gravity is exceeded.

Example 15–5. A centrifuge is rotating at 1500 rpm. The midpoint of the cell containing the sample is located 7.5 cm from the center of the rotor (i.e., $x = 7.5$ cm). What is the average angular acceleration and the number of "g"s on the suspended particles?

$$\text{Angular acceleration} = \omega^2 x$$
$$= \left(\frac{1500 \text{ revolutions}}{\text{minute}} \times \frac{2\pi}{60}\right)^2 \times 7.5 \text{ cm}$$
$$= 1.851 \times 10^5 \text{ cm/sec}^2$$
$$\text{Number of "g"s} = \frac{1.851 \times 10^5 \text{ cm/sec}^2}{981 \text{ cm/sec}^2}$$
$$= 188.7 \text{ "g"s}$$

that is, the force produced is 188.7 times that due to gravity.

The instantaneous velocity $v = dx/dt$ of a particle in a unit centrifugal field is expressed in terms of the *Svedberg sedimentation coefficient* s,

$$s = \frac{dx/dt}{\omega^2 x} \qquad (15-15)$$

Owing to the centrifugal force, particles having a high molecular weight pass from position x_1 at time t_1 to position x_2 at time t_2, and the sedimentation coefficient is obtained by integrating equation (15–15) to give

$$s = \frac{\ln (x_2/x_1)}{\omega^2(t_2 - t_1)} \qquad (15-16)$$

The distances x_1 and x_2 refer to positions of the boundary between the solvent and the high-molecular-weight component in the centrifuge cell. The boundary is located by the change of refractive index, which may be attained at any time during the run and translated into a peak on a photographic plate. Photographs are taken at definite intervals, and the peaks of the

schlieren patterns, as they are called, give the position x of the boundary at each time, t. If the sample consists of a component of a definite molecular weight, the schlieren pattern will have a single sharp peak at any moment during the run. If components with different molecular weights are present in the sample, the particles of greater weight will settle faster, and several peaks will appear on the schlieren patterns. Therefore, ultracentrifugation is useful not only for determining the molecular weight of polymers, particularly proteins, but also may be used to ascertain the degree of homogeneity of the sample. Gelatin, for example, is found to be a polydisperse protein with fractions of molecular weight 10,000 to 100,000. (This accounts in part for the fact that gelatin from various sources is observed to have variable properties when used in pharmaceutical preparations.) Insulin, on the other hand, is a monodisperse protein composed of two polypeptide chains, each made up of a number of amino acid molecules. The two chains are attached together by disulfide—S—S— bridges to form a definite unit having a molecular weight of about 6000.

The sedimentation coefficient s may be computed from equation (15–16) after the two distances x_1 and x_2 are measured on the schlieren photographs obtained at times t_1 and t_2; the angular velocity ω is equal to 2π times the speed of the rotor in revolutions per second. Knowing s and obtaining D from diffusion data, it is possible to determine the molecular weight of a polymer, such as a protein, by use of the expression

$$M = \frac{RTs}{D(1 - \bar{v}\rho_o)} \qquad (15\text{–}17)$$

in which R is the molar gas constant, T is the absolute temperature, $\bar{v}$ is the partial specific volume of the protein, and ρ_o is the density of the solvent. Both s and D must be obtained at, or corrected to, 20° C for use in equation (15–17).

Example 15–6. The sedimentation coefficient s for a particular fraction of methylcellulose at 20° C (293° K) is 1.7×10^{-13} sec, the diffusion coefficient D is 15×10^{-7} cm²/sec, the partial specific volume $\bar{v}$ of the gum is 0.72cm³/g, and the density of water at 20° C is 0.998 g/cm³. Compute the molecular weight of methylcellulose. The gas constant R is 8.31×10^7 erg/(deg mole).

$$M = \frac{(8.31 \times 10^7) \times 293 \times (1.7 \times 10^{-13})}{15 \times 10^{-7}[1 - (0.72 \times 0.998)]}$$

$$= 9800 \text{ g/mole}$$

Kirschbaum[8] has reviewed the usefulness of the analytic ultracentrifuge and has used it to study the micellar properties of drugs (Fig. 15–8*a*, *b*). Richard [9] determined the apparent micellar molecular weight of the antibiotic fusidate sodium by ultracentrifugation. He concluded the primary micelles composed of five monomer units are formed, followed by aggregation of these pentamers into larger micelles at higher salt concentrations.

The sedimentation method already described is known as the *sedimentation velocity* technique. A second method, involving *sedimentation equilibrium*, may also be used. Equilibrium is established when the sedimentation force is just balanced by the counteracting diffusional force and the boundary is therefore stationary. In this method, the diffusion coefficient need not be determined; however, the centrifuge may have to be run for several weeks to attain equilibrium throughout the cell. Newer methods of calculation have been developed recently for obtaining molecular weights by the equilibrium method without requiring these long periods of centrifugation, enabling the

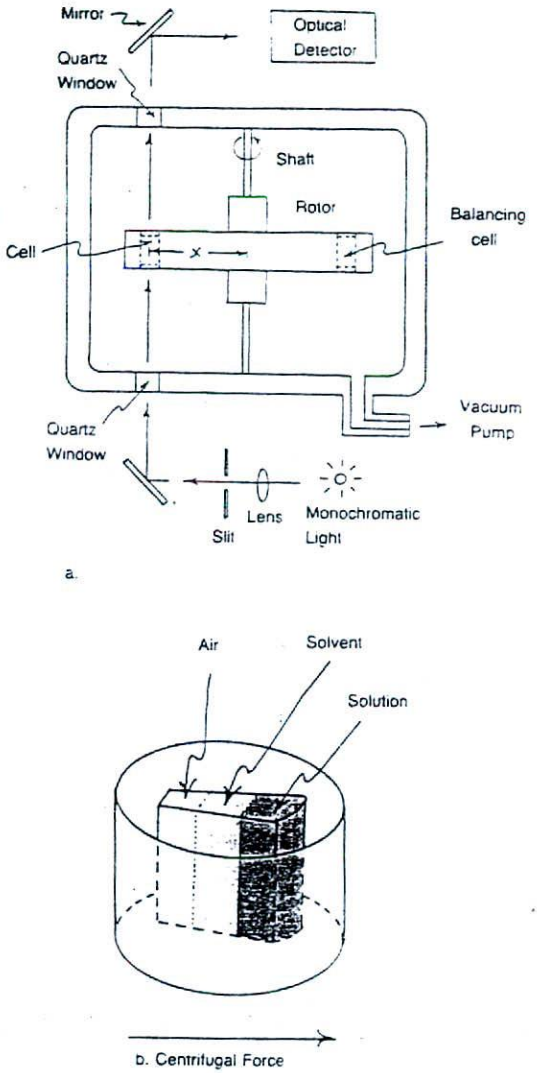

Fig. 15–8. (*a*) Schematic of the ultracentrifuge. (*b*) Centrifuge cell. (From H. R. Allcock and F. W. Lampe, *Contemporary Polymer Chemistry*, Prentice-Hall, Englewood Cliffs, N.J., 1981, pp. 366, 367, reproduced with permission of the copyright owner.)

protein chemist to obtain molecular weights rapidly and accurately.

Molecular weights determined by sedimentation velocity, sedimentation equilibrium, and osmotic pressure determinations are in good agreement, as may be seen from Table 15–4.

Viscosity. Viscosity is an expression of the resistance to flow of a system under an applied stress. The more viscous a liquid, the greater the applied force required to make it flow at a particular rate. The fundamental principles and applications of viscosity are discussed in detail in Chapter 17. The present section is concerned with the flow properties of dilute colloidal systems and the manner in which viscosity data can be used to obtain the molecular weight of material comprising the disperse phase. Viscosity studies also provide information regarding the shape of the particles in solution.

Einstein developed an equation of flow applicable to dilute colloidal dispersions of spherical particles, namely,

$$\eta = \eta_o(1 + 2.5\phi) \qquad (15-18)$$

In equation (15–18), which is based on hydrodynamic theory, η_o is the viscosity of the dispersion medium and η is the viscosity of the dispersion when the volume fraction of colloidal particles present is ϕ. The volume fraction is defined as the volume of the particles divided by the total volume of the dispersion; it is therefore equivalent to a concentration term. Both η_o and η may be determined using a capillary viscometer, described on pp. 461–462.

Several viscosity coefficients may be defined with respect to this equation. These include *relative viscosity*, *specific viscosity* (η_{sp}), and *intrinsic viscosity* [η]. From equation (15–18),

$$\eta_{rel} = \frac{\eta}{\eta_o} = 1 + 2.5\phi \qquad (15-19)$$

and

$$\eta_{sp} = \frac{\eta}{\eta_o} - 1 = \frac{\eta - \eta_o}{\eta_o} = 2.5\phi \qquad (15-20)$$

TABLE 15–4. ***Molecular Weights of Proteins in Aqueous Solution****

Material	Molecular Weight		
	Sedimentation Velocity	Sedimentation Equilibrium	Osmotic Pressure
Ribonuclease	12,700	13,000	—
Myoglobin	16,900	17,500	17,000
Ovalbumin	44,000	40,500	45,000
Hemoglobin (horse)	68,000	68,000	67,000
Serum albumin (horse)	70,000	68,000	73,000
Serum globulin (horse)	167,000	150,000	175,000
Tobacco mosaic virus	59,000,000	—	—

*From D. J. Shaw, *Introduction to Colloid and Surface Chemistry*, Butterworths, London, 1970, p. 32. For an extensive listing of molecular weights of macromolecules, see C. Tanford, *Physical Chemistry of Macromolecules*, Wiley, New York, 1961.

or

$$\frac{\eta_{sp}}{\phi} = 2.5 \qquad (15-21)$$

Since volume fraction is directly related to concentration, equation (15–21) may be written as

$$\frac{\eta_{sp}}{c} = k \qquad (15-22)$$

in which c is expressed in grams of colloidal particles per 100 mL of total dispersion. For highly polymeric materials dispersed in the medium at moderate concentrations, the equation is best expressed as a power series:

$$\frac{\eta_{sp}}{c} = k_1 + k_2c + k_3c^2 \qquad (15-23)$$

By determining η at various concentrations and knowing η_o, η_{sp} can be calculated from equation (15–20). If η_{sp}/c is plotted against c (see Fig. 15–9, and the line extrapolated to infinite dilution, the intercept is k_1 (equation [15–23]). This constant, commonly known as the intrinsic viscosity, [η], is used to calculate the approximate molecular weights of polymers. According to the Mark–Houwink equation,

$$[\eta] = KM^a \qquad (15-24)$$

in which K and a are constants characteristic of the particular polymer–solvent system. These constants, which are virtually independent of molecular weight, are obtained initially by determining [η] experimentally for polymer fractions whose molecular weights have been determined by other methods such as light scattering, osmotic pressure, or sedimentation. Once K and a are known, measurement of [η] provides a simple yet accurate means of obtaining molecular weights for fractions not yet subjected to other methods. The details of the calculation are brought out by working through Problem 15–19. Intrinsic viscosity [η], together with an interaction constant k', provides an equation, $\eta_{sp}/c = [\eta] + k'[\eta]^2c$, for use to choose solvent

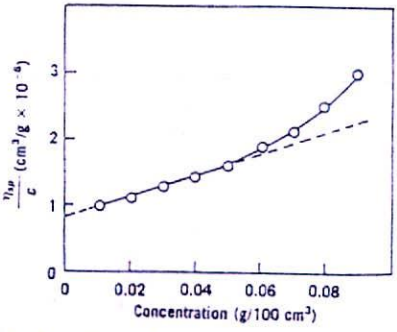

Fig. 15–9. Determination of molecular weight using viscosity data. (D. R. Powell J. Swarbrick and G. S. Banker, J. Pharm. Sci. 55, 601, 1966, reproduced with permission of copyright owner.)

mixtures for tablet film coating polymers such as ethyl cellulose.[10]

The viscosity of colloidal dispersions is affected by the shapes of particles of the disperse phase. Spherocolloids form dispersions of relatively low viscosity, while systems containing linear particles are more viscous. As we have seen in previous sections, the relationship of shape and viscosity reflects the degree of solvation of the particles. If a linear colloid is placed in a solvent for which it has a low affinity, it tends to "ball up," that is, to assume a spherical shape, and the viscosity falls. This provides a means of detecting changes in the shape of flexible colloidal particles and macromolecules.

The characteristics of polymers used as substitutes for blood plasma (plasma extenders) depend in part on the molecular weight of the material. These characteristics include the size and shape of the macromolecules and the ability of the polymers to impart the proper viscosity and osmotic pressure to the blood. The methods described in this chapter are used to determine the average molecular weights of hydroxyethyl starch, dextran, and gelatin preparations used as plasma extenders. Ultracentrifugation, light scattering, x-ray analysis (small-angle x-ray scattering[11]), and other analytic tools[12] were used by Paradies to determine the structural properties of tyrothricin, a mixture of the peptide antibiotics gramicidine and tyrocidine B. The antibiotic aggregate has a molecular weight of 28,600 daltons and was determined to be a rod of 170 Å in length and 30 Å in diameter.

ELECTRIC PROPERTIES OF COLLOIDS

The properties of colloids that depend on, or are affected by, the presence of a charge on the surface of a particle are discussed under this heading. The various ways in which the surface of particles dispersed in a liquid medium acquire a charge has already been outlined in Chapter 14 (which treated interfacial phenomena) (p. 386). Mention was also made of the *zeta (electrokinetic)* potential and how it is related to the *Nernst (electrothermodynamic)* potential. The potential versus distance diagram for a spherical colloidal particle may be represented as shown in Figure 15–10. Such a system may be formed, for example, by adding

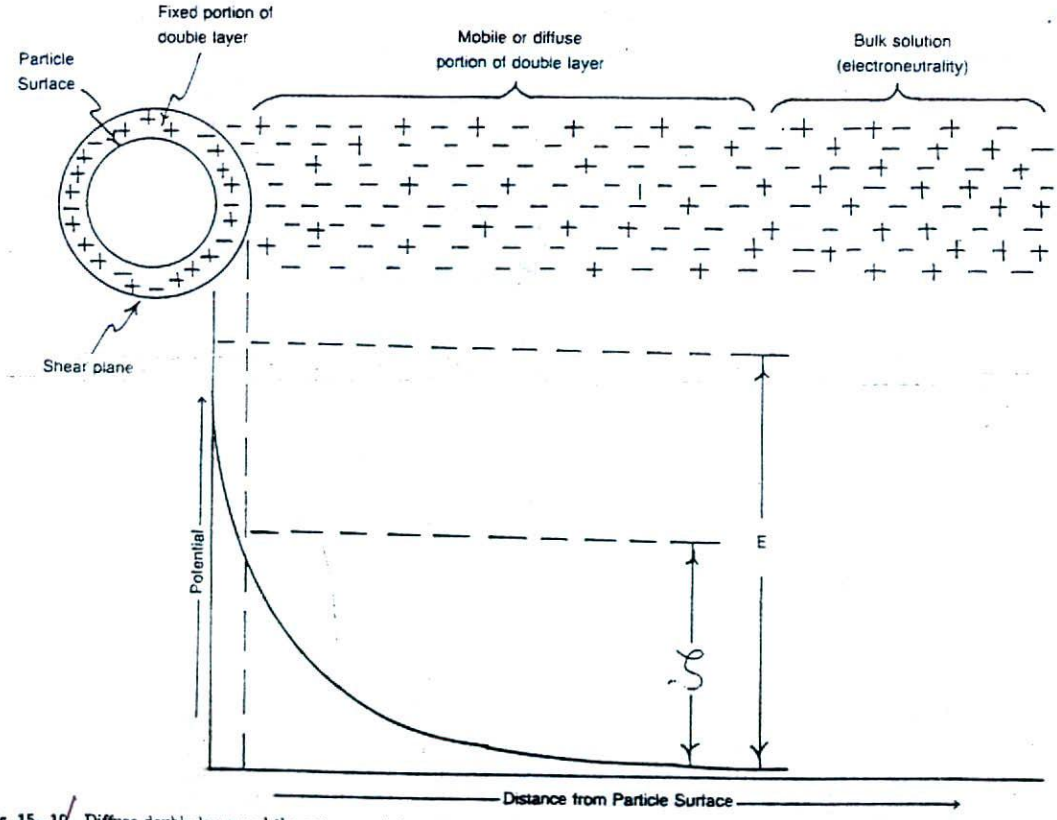

Fig. 15–10. Diffuse double layer and the zeta potential.

a dilute solution of potassium iodide to an equimolar solution of silver nitrate. A colloidal precipitate of silver iodide particles is produced and, because the silver ions are in excess and are adsorbed, a positively charged particle is produced. If the reverse procedure is adopted, that is, if silver nitrate is added to the potassium iodide solution, iodide ions are adsorbed on the particles as the potential-determining ion and result in the formation of a negatively charged sol.

Electrokinetic Phenomena. The movement of a charged surface with respect to an adjacent liquid phase is the basic principle underlying four electrokinetic phenomena: *electrophoresis*, *electroosmosis*, *sedimentation potential*, and *streaming potential*.

Electrophoresis involves the movement of a charged particle through a liquid under the influence of an applied potential difference. An electrophoresis cell, fitted with two electrodes, contains the dispersion. When a potential is applied across the electrodes, the particles migrate to the oppositely charged electrode. Figure 15–11 illustrates the design of a commercially available instrument. The rate of particle migration is observed by means of an ultramicroscope and is a function of the charge on the particle. As the shear plane of the particle is located at the periphery of the tightly bound layer, the rate-determining potential is the zeta potential. From a knowledge of the direction and rate of migration, the sign and magnitude of the zeta potential in a colloidal system may be determined. The relevant equation

$$\zeta = \frac{v}{E} \times \frac{4\pi\eta}{\epsilon} \times (9 \times 10^4) \qquad (15\text{–}25)$$

which yields the zeta potential (ζ) in volts, requires a knowledge of the velocity of migration v of the sol in cm/sec in an electrophoresis tube of a definite length in cm, the viscosity of the medium η in poises (dyne sec/cm^2), the dielectric constant of the medium ϵ, and the potential gradient E in volts/cm. The term v/E is known as the *mobility*.

It is instructive to carry out the dimensional analysis of equation (15–25). In one system of fundamental electric units, E, the electric field strength, can be expressed in electrostatic units of statvolt/cm (a coulomb is equal to 3×10^9 statcoulombs, and 1 statvolt equals 300 practical volts). The dielectric constant is not dimensionless here, but rather from Coulomb's law may be assigned the units of statcoulomb^2/(dyne cm^2). The equation

$$\zeta = \frac{v}{E} \frac{4\pi\eta}{\epsilon} \qquad (15\text{–}26)$$

may then be written dimensionally, recognizing that statvolts × statcoulombs = dyne cm, as

$$\zeta = \frac{\text{cm/sec}}{\text{statvolts/cm}} \times \frac{\text{dyne sec/cm}^2}{\text{statcoulomb}^2/(\text{dyne cm}^2)} = \text{statvolts} \qquad (15\text{–}27)$$

It is more convenient to express zeta potential in practical volts that in statvolts. Since 1 statvolt is equal to 300 practical volts, equation (15–27) is multiplied by 300 to make this conversion, that is, statvolts × 300 practical volts/statvolt = 300 practical volts. Furthermore, E is ordinarily measured in practical volts/cm and not in statvolt/cm, and this conversion is made by again multiplying the right-hand side of equation (15–27) by 300. The final expression is equation (15–25), in which the factor, $300 \times 300 = 9 \times 10^4$, converts electrostatic units to volts.

For a colloidal system at 20° C in which the dispersion medium is water, equation (15–25) reduces approximately to

$$\zeta \cong 141 \frac{v}{E} \qquad (15\text{–}28)$$

The coefficient, 141, at 20° C becomes 128 at 25° C.

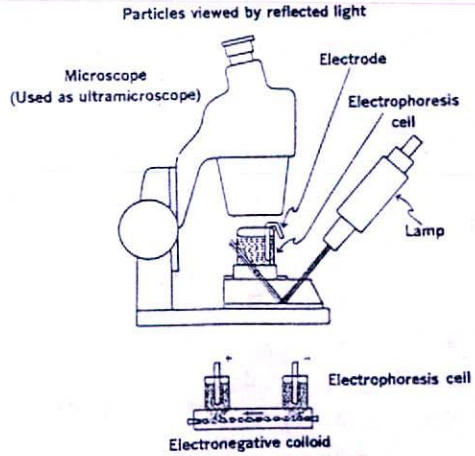

Fig. 15–11. Principle of zeta potential measurement (based on Zeta Meter) showing ultramicroscope and flow cell.

Example 15–7. The velocity of migration of an aqueous ferric hydroxide sol was determined at 20° C using the apparatus shown in Figure 15–11 and was found to be 16.5×10^{-4} cm/sec. The distance between the electrodes in the cell was 20 cm, and the applied emf was 110 volts. What is (*a*) the zeta potential of the sol and (*b*) the sign of the charge on the particles?

(*a*)

$$\frac{v}{E} = \frac{16.5 \times 10^{-4} \text{ cm/sec}}{110/20 \text{ volts/cm}} = 3 \times 10^{-4} \text{ cm}^2 \text{ volt}^{-1} \text{ sec}^{-1}$$

$$\zeta = 141 \times (3 \times 10^{-4}) = 0.042 \text{ volt}$$

(*b*) The particles were seen to migrate toward the negative electrode of the electrophoresis cell; therefore, the colloid is positively charged. The zeta potential is often used to estimate the stability of colloids, as discussed in a later section.

Electroosmosis is essentially the opposite in principle to that of electrophoresis. In the latter, the

application of a potential causes a charged particle to move relative to the liquid, which is stationary. If the solid is rendered immobile (i.e., by forming a capillary or making the particles into a porous plug), however, the liquid now moves relative to the charged surface. This is electroosmosis, so called because liquid moves through a plug or membrane across which a potential is applied. Electroosmosis provides another method for obtaining zeta potential by determining the rate of flow of liquid through the plug under standard conditions.

Sedimentation potential, the reverse of electrophoresis, is the creation of a potential when particles undergo sedimentation. *Streaming potential* differs from electroosmosis in that the potential is created by forcing a liquid to flow through a plug or bed of particles.

Schott[13] studied the electrokinetic properties of magnesium hydroxide suspensions that are used as antacids and laxatives. The zero point of charge occurred at pH ≅ 10.8, the zeta potential, ζ, of magnesium hydroxide being positive below this pH value. Increasing the pH or hydroxide ion concentration produced a change in the sign of ζ from positive to negative, with the largest negative ζ value occurring at pH 11.5.

Takenaka and associates[14] studied the electrophoretic properties of *microcapsules* (pp. 516–517) of sulfamethoxazole in droplets of a gelatin–acacia coacervate as part of a study to stabilize such drugs in microcapsules.

Crommelin[15] determined the effect of adding charge-inducing agents such as stearylamine or phosphatidylserine on the zeta potential of liposomes (p. 513) of phosphatidylcholine and cholesterol in aqueous media. The physical stability of the liposomes was predicted on the basis of the Derjaguin–Landau–Verwey–Overbeek (DLVO) theory (p. 408). The physical stability predicted from the theory did not, however, correlate with the experimentally obtained stability.

Schott and Young[16] determined the electrophoretic mobility of the gram-positive *Streptococcus faecalis* and the gram-negative *Escherichia coli* as a function of ionic strength and pH. An increase in concentration of buffer electrolytes (increased ionic strength) reduced the mobility, u_E, of *S. faecalis*. Both *E. coli* and *S. faecalis* were negatively charged over the pH range studied. The chemical group responsible for the charge at the surface of both bacteria presumably is the carboxyl group.

The magnitude and sign of the electric charge of ampholytic drugs (p. 149) at physiologic pH influences their absorption from the gastrointestinal tract and their passage through bacterial membranes. Schott and Astigarrabia[17] determined the isoelectric points (p. 149) of four very slightly soluble sulfonamides by electrophoresis of their suspensions as a function of pH. The isoelectric points of all four sulfonamides were between 3.5 and 4.6, indicating that the sulfonamides are weak acids rather than zwitterions at the normal physiologic pH of 7.4.

Donnan Membrane Equilibrium. If sodium chloride is placed in solution on one side of a semipermeable membrane, and a negatively charged colloid, together with its counterions R^-Na^+, is placed on the other side, the sodium and chloride ions can pass freely across the barrier but not the colloidal anionic particles. The system at equilibrium is represented in the following diagram, in which R^- is the nondiffusible colloidal anion and the vertical line separating the various species represents the semipermeable membrane. The volumes of solution on the two sides of the membrane are considered to be equal.

outside (o)	inside (i)
	R^-
Na^+	Na^+
Cl^-	Cl^-

After equilibrium has been established, the concentration in dilute solutions (more correctly the activity) of sodium chloride must be the same on both sides of the membrane, according to the principle of escaping tendencies (p. 106). Therefore,

$$[Na^+]_o[Cl^-]_o = [Na^+]_i[Cl^-]_i \qquad (15\text{–}29)$$

The condition of electroneutrality must also apply. That is, the concentration of positively charged ions in the solutions on either side of the membrane must balance the concentration of negatively charged ions. Therefore, on the outside,

$$[Na^+]_o = [Cl^-]_o \qquad (15\text{–}30)$$

and inside,

$$[Na^+]_i = [R^-]_i + [Cl^-]_i \qquad (15\text{–}31)$$

Equations (15–30) and (15–31) may be substituted into (15–29) to give

$$[Cl^-]_o^2 = ([Cl^-]_i + [R^-]_i)[Cl^-]_i$$

$$= [Cl^-]_i^2\left(1 + \frac{[R^-]_i}{[Cl^-]_i}\right) \qquad (15\text{–}32)$$

$$\frac{[Cl^-]_o}{[Cl^-]_i} = \sqrt{1 + \frac{[R^-]_i}{[Cl^-]_i}} \qquad (15\text{–}33)$$

Equation (15–33), the *Donnan membrane equilibrium*, gives the ratio of concentrations of the diffusible anion outside and inside the membrane at equilibrium. The equation shows that a negatively charged polyelectrolyte inside a semipermeable sac would influence the equilibrium concentration ratio of a diffusible anion. It tends to drive the ion of like charge out through the membrane. When $[R^-]_i$ is large compared with $[Cl^-]_i$, the ratio roughly equals $\sqrt{[R^-]_i}$. If, on the other hand, $[Cl^-]_i$ is quite large with respect to $[R^-]_i$, the ratio in equation (15–33) becomes equal to unity, and the

concentration of the salt is thus equal on both sides of the membrane.

The unequal distribution of diffusible electrolyte ions on the two sides of the membrane will obviously result in erroneous values for osmotic pressures of polyelectrolyte solutions. If, however, the concentration of salt in the solution is made large, the Donnan equilibrium effect can be practically eliminated in the determination of molecular weights of proteins involving the osmotic pressure method.

Higuchi et al.[18] modified the Donnan membrane equilibrium, equation (15–33), to demonstrate the use of the polyelectrolyte sodium carboxymethylcellulose for enhancing the absorption of drugs such as sodium salicylate and potassium benzylpenicillin. If $[Cl^-]$ in equation (15–33) is replaced by the concentration of the diffusible drug, anion $[D^-]$ at equilibrium, and $[R^-]$ is used to represent the concentration of sodium carboxymethylcellulose at equilibrium, we have a modification of the *Donnan membrane equilibrium* for a diffusible drug anion, $[D^-]$:

$$\frac{[D^-]_o}{[D^-]_i} = \sqrt{1 + \frac{[R^-]_i}{[D^-]_i}} \qquad (15\text{–}34)$$

It will be observed that when $[R^-]_i/[D^-]_i = 8$, the ratio $[D^-]_o/[D^-]_i = 3$, and when $[R^-]_i/[D^-]_i = 99$, the ratio $[D^-]_o/[D^-]_i = 10$. Therefore, the addition of an anionic polyelectrolyte to a diffusible drug anion should enhance the diffusion of the drug out of the chamber. By kinetic studies, Higuchi et al.[18] showed that the presence of sodium carboxymethylcellulose more than doubled the rate of transfer of the negatively charged dye, scarlet red sulfonate.

Other investigators have found by in vivo experiments that ion-exchange resins and even sulfate and phosphate ions that do not diffuse readily through the intestinal wall, tend to drive anions from the intestinal tract into the bloodstream. The opposite effect, that of retardation of drug absorption, may occur if the drug complexes with the macromolecule.

Example 15–8. A solution of dissociated nondiffusible carboxymethylcellulose is equilibrated across a semipermeable membrane with a solution of sodium salicylate. The membrane allows free passage of the salicylate ion. Compute the ratio of salicylate on the two sides of the membrane at equilibrium, assuming that the equilibrium concentration of carboxymethylcellulose is 1.2×10^{-2} gram equivalent/liter and the equilibrium concentration of sodium salicylate is 6.0×10^{-3} gram equivalent/liter. The modified Donnan membrane expression, equation (15–34), is used:

$$\frac{[D^-]_o}{[D^-]_i} = \sqrt{1 + \frac{[R^-]}{[D^-]_i}}$$

$$= \sqrt{1 + \frac{12 \times 10^{-3}}{6 \times 10^{-3}}} = 1.73$$

Stability of Colloid Systems. The presence and magnitude, or absence, of a charge on a colloidal particle is an important factor in the stability of colloidal systems. Stabilization is accomplished essentially by two means: providing the dispersed particles with an electric charge, and surrounding each particle with a protective solvent sheath that prevents mutual adherence when the particles collide as a result of Brownian movement. This second effect is significant only in the case of lyophilic sols.

A lyophobic sol is thermodynamically unstable. The particles in such sols are stabilized only by the presence of electric charges on their surfaces. The like charges produce a repulsion that prevents coagulation of the particles. If the last traces of ions are removed from the system by dialysis, the particles can agglomerate and reduce the total surface area, and, owing to their increased size, they may settle rapidly from suspension. Hence, addition of a small amount of electrolyte to a lyophobic sol tends to stabilize the system by imparting a charge to the particles. Addition of electrolyte beyond that necessary for maximum adsorption on the particles, however, sometimes results in the accumulation of opposite ions and reduces the zeta potential below its *critical value*. The critical potential for finely dispersed oil droplets in water (oil hydrosol) is about 40 millivolts, this high value signifying relatively great instability. The critical zeta potential of a gold sol, on the other hand, is nearly zero, which suggests that the particles require only a minute charge for stabilization; hence, they exhibit marked stability against added electrolytes. The valence of the ions having a charge opposite to that of the particles appears to determine the effectiveness of the electrolyte in coagulating the colloid. The precipitating power increases rapidly with the valence or charge of the ions, and a statement of this fact is known as the *Schulze–Hardy rule*.

These observations permitted Verwey and Overbeek[19] and Derjaguin and Landau[20] to independently develop a theory that describes the stability of lyophobic colloids. According to this approach, known as the DLVO theory, the forces on colloidal particles in a dispersion are due to electrostatic repulsion and London-type van der Waal's attraction. These forces result in potential energies of repulsion, V_R, and attraction, V_A, between particles. These are shown in Figure 15–12 together with the curve for the composite potential energy, V_T. There is a deep potential "well" of attraction near the origin and a high potential barrier of repulsion at moderate distances. A shallow secondary trough of attraction (or minimum) is sometimes observed at longer distances of separation. The presence of a secondary minimum is significant in the controlled flocculation of coarse dispersions (see Chapter 18). Following this principle, one can determine somewhat quantitatively the amount of electrolyte of a particular valence type required to precipitate a colloid.

Not only do electrolytes bring about coagulation of colloidal particles; the mixing of oppositely charged colloids can also result in mutual agglomeration.

Lyophilic and association colloids are thermodynamically stable and exist in true solution so that the system constitutes a single phase. The addition of an electrolyte to a lyophilic colloid in moderate amounts does not

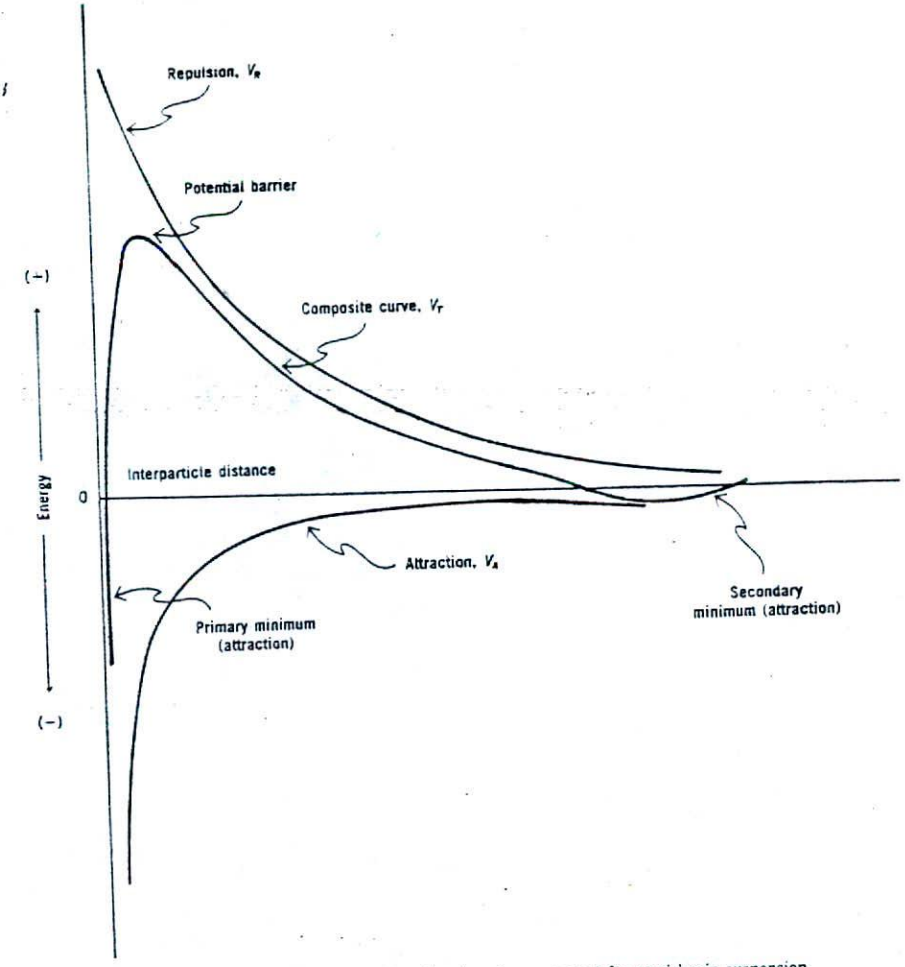

Fig. 15–12. Potential energy versus interparticle distance (usually given in angstroms) for particles in suspension.

result in coagulation, as was evident with lyophobic colloids. If sufficient salt is added, however, agglomeration and sedimentation of the particles may result. This phenomenon, referred to as "salting-out," was discussed in the chapter on solubility.

Just as the Schulze–Hardy rule arranges ions in the order of their capacity to coagulate hydrophobic colloids, the *Hofmeister* or *lyotropic series* ranks cations and anions in order of coagulation of hydrophilic sols. Several anions of the Hofmeister series in decreasing order of precipitating power are citrate, tartrate, sulfate, acetate, chloride, nitrate, bromide, and iodide. The precipitating power is directly related to the hydration of the ion and hence to its ability to separate water molecules from the colloidal particles.

Alcohol and acetone can also decrease the solubility of hydrophilic colloids so that the addition of a small amount of electrolytes may then bring about coagulation. The addition of the less polar solvent renders the solvent mixture unfavorable for the colloid, and electrolytes can then salt out the colloid with relative ease. We may thus regard flocculation on the addition of alcohol, followed by salts, as a gradual transformation from a sol of a lyophilic nature to one of a more lyophobic character.

When negatively and positively charged hydrophilic colloids are mixed, the particles may separate from the dispersion to form a layer rich in the colloidal aggregates. The colloid-rich layer is known as a *coacervate*, and the phenomenon in which macromolecular solutions separate into two liquid layers is referred to as *coacervation*. As an example, consider the mixing of gelatin and acacia. Gelatin at a pH below 4.7 (its isoelectric point) is positively charged; acacia carries a

negative charge that is relatively unaffected by pH in the acid range. When solutions of these colloids are mixed in a certain proportion, coacervation results. The viscosity of the upper layer, now poor in colloid, is markedly decreased below that of the coacervate, and in pharmacy this is considered to represent a physical incompatibility. Coacervation need not involve the interaction of charged particles; the coacervation of gelatin may also be brought about by the addition of alcohol, sodium sulfate, or a macromolecular substance such as starch.

Takenaka et al.[21] microencapsulated (p. 516) sulfamethoxazole in a gelatin–acacia coacervate, and reported on the particle size, wall thickness, and porosity of the microcapsules.

Badawi and El-Sayed[22] investigated the equilibrium solubility and dissolution rate of a coacervate of sulfathiazole complexed with povidone. They found the dissolution rate to be enhanced by coacervation. In forming the coacervate, an amorphous precipitate is formed when the sulfonamide is treated by acid or base in aqueous solution or when an alcoholic solution of the drug is diluted with water. In the presence of povidone a complex is formed with the partially precipitated sulfathiazole, resulting in a coacervate. The addition of resorcinol, a coacervating agent for povidone, to an aqueous mixture of sulfathiazole sodium and povidone also resulted in coacervation.

Sensitization and Protective Colloidal Action. The addition of a small amount of hydrophilic or hydrophobic colloid to a hydrophobic colloid of opposite charge tends to sensitize or even coagulate the particles. This is considered by some workers to be due to a reduction of the zeta potential below the critical value (usually about 20 to 50 millivolts). Others attribute the instability of the hydrophobic particles to a reduction in the thickness of the ionic layer surrounding the particles and a decrease in the coulombic repulsion between the particles. The addition of large amounts of the *hydrophile* (hydrophilic colloid), however, stabilizes the system, the hydrophile being adsorbed on the hydrophobic particles. This phenomenon is known as *protection*, and the added hydrophilic sol is known as a *protective colloid*. The several ways in which stabilization of hydrophobic colloids can be achieved (i.e., protective action) have been reviewed by Schott.[23]

The protective property is expressed most frequently in terms of the *gold number*. The gold number is the minimum weight in milligrams of the protective colloid (dry weight of dispersed phase) required to prevent a color change from red to violet in 10 mL of a gold sol on the addition of 1 mL of a 10% solution of sodium chloride. The gold numbers for some common protective colloids are given in Table 15–5.

A pharmaceutical example of sensitization and protective action is provided when bismuth subnitrate is suspended in a tragacanth dispersion; the mixture forms a gel that sets to a hard mass in the bottom of the container. Bismuth subcarbonate, a compound that does not dissociate sufficiently to liberate the bismuth ions, is compatible with tragacanth.

TABLE 15–5. *The Gold Number of Protective Colloids*

Protective Colloid	Gold Number
Gelatin	0.005–0.01
Albumin	0.1
Acacia	0.1–0.2
Sodium oleate	1–5
Tragacanth	2

These phenomena probably involve a sensitization and coagulation of the gum by the Bi^{3+} ions. The flocculated gum then aggregates with the bismuth subnitrate particles to form a gel or a hard cake. If phosphate, citrate, or tartrate are added, they protect the gums from the coagulating influence of the Bi^{3+} ions, and, no doubt, by reducing the zeta potential on the bismuth particles, partially flocculate the insoluble material. Partially flocculated systems tend to cake considerably less than deflocculated systems, and this effect is significant in the formulation of suspensions[24] (Chapter 18).

SOLUBILIZATION

An important property of association colloids in solution is the ability of the micelles to increase the solubility of materials that are normally insoluble, or only slightly soluble, in the dispersion medium used. This phenomenon, known as *solubilization*, has been reviewed by many authors including Mulley,[25] Nakagawa,[26] Elworthy and coauthors,[27] and Attwood and Florence.[28] Solubilization has been used with advantage in pharmacy for many years; as early as 1892, Engler and Dieckhoff[29] solubilized a number of compounds in soap solutions.

Knowing the location, distribution, and orientation of solubilized drugs in the micelle is important to understanding the kinetic aspect of the solubilization process and the interaction of drugs with the different elements that constitute the micelle. These factors may also affect the stability and bioavailability of the drug. The location of the molecule undergoing solubilization in a micelle is related to the balance between the polar and nonpolar properties of the molecule. Lawrence[30] was the first to distinguish between the various sites. He proposed that nonpolar molecules in aqueous systems of ionic surface-active agents would be located in the hydrocarbon core of the micelle, while polar solubilizates would tend to be adsorbed onto the micelle surface. Polar–nonpolar molecules would tend to align themselves in an intermediate position within the surfactant molecules forming the micelle. Nonionic surfactants are of most pharmaceutical interest as solubilizing agents because of their lower toxicity.

Their micelles show a gradient of increased polarity from the core to the polyoxyethylene–water surface. The extended interfacial region between the core and the aqueous solution, that is, the polar mantle, is greatly hydrated. The anisotropic distribution of water molecules within the polar mantle favors the inclusion (solubilization) of a wide variety of molecules.[31] Solubilization may therefore occur in both the core and the mantle, also called the *palisade layer*. Thus, certain compounds (e.g., phenols and related compounds with a hydroxy group capable of bonding with the ether oxygen of the polyoxyethylene group) are held between the polyoxyethylene chains. Under these conditions, such compounds may be considered as undergoing inclusion within the polyoxyethylene exterior of the micelle rather than adsorption onto the micelle surface. Figure 15–13 depicts a spherical micelle of a nonionic, polyoxyethylene monostearate, surfactant in water. The figure is drawn in conformity with Reich's suggestion[32] that such a micelle may be regarded as a hydrocarbon core, made up of the hydrocarbon chains of the surfactant molecules, surrounded by the polyoxyethylene chains protruding into the continuous aqueous phase. Benzene and toluene, nonpolar molecules, are shown solubilized in the hydrocarbon interior of the micelle. Salicylic acid, a more polar molecule, is oriented with the nonpolar part of the molecule directed toward the central region of the micelle and the polar group toward the hydrophilic chains that spiral outward into the aqueous medium. Parahydroxybenzoic acid, a predominantly polar molecule, is found completely between the hydrophilic chains.

Nuclear magnetic resonance (NMR) and spectroscopic imaging techniques employing the visible and ultraviolet regions of the spectrum are used to establish the site of solubilization. Some ultraviolet spectroscopic

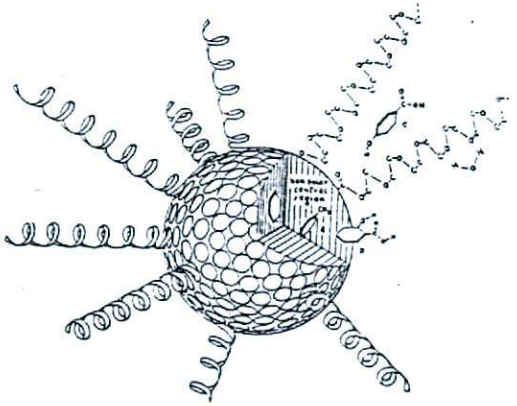

Fig. 15–13. Artist's conception of a spherical micelle of nonionic surfactant molecules. (*a*) A nonpolar molecule solubilized in the nonpolar region of the micelle. (*b*) A more polar molecule found partly embedded in the central region and partly extending into the palisade region. (*c*) A polar molecule found lying well out in the palisade layer attracted by dipolar forces to the polyoxyethylene chains.

characteristics are sensitive to the polarity of the medium. Thus the spectral shifts of compounds solubilized in micelles are used to determine the microenvironmental polarity of their sites of solubilization. Mukerjee and coworkers[33,34] determined the dielectric constant D of the microenvironment of benzene solubilized both in sodium dodecyl sulfate, an anionic surfactant, and in cetyltrimethylammonium chloride, a cationic surfactant. The results of the dielectric constant study show quite polar and similar microenvironments (D = 40) in the two micelles of different charge type, suggesting that benzene is mainly located at the surface, that is, in the polar part of the micelle rather than in the core.

These researchers[33,34] proposed a *two-state model* of solubilization. The less polar state involves the hydrocarbon core and is called the *dissolved state*. The other region is the micelle–water interface, the *adsorbed state*, where the environment is more polar. In this model, the total solubilizing power of a micelle is the sum of the "adsorbed" fraction and the "dissolved" fraction of solubilizate. When adsorption occurs, the solubilization is increased beyond that can be attributed alone to the solvent power of the core. Another interesting finding predicted by the model is that the microenvironmental polarity of solubilizate shows little dependence on the kind of charge on the micelle. The equilibrium between the "adsorbed" and "dissolved" states can be assumed to be similar to that in bulk systems such as in the immiscible liquid pair dodecane–water. Thus, a quantitative estimate of the solvent power of the hydrocarbon core for the solubilizate can be obtained from the dodecane–water partition coefficient of the solubilizate.

However, for a more detailed picture, the core is subjected to a substantial *Laplace pressure*, which reduces its solvent power as compared with dodecane. The Laplace pressure P is due to the curved interface and is given by the relation (p. 365)

$$P = 2\gamma/r \qquad (15\text{–}35)$$

where γ is the interfacial tension and r is the radius of the micelle. The pressure P opposes the entry of all guest molecules to be solubilized. The factor χ by which the solubility is reduced is related to the partial molar volume of the solubilizate according to the relationship[33,34]

$$P\bar{v} = RT \ln \chi \qquad (15\text{–}36)$$

Equation (15–36) indicates that χ varies exponentially with P and therefore with $1/r$ when surface tension, γ, is constant. Using equation (15–36) and knowing K, the dodecane–water distribution coefficient, it is possible to estimate the partitioning of a solubilizate between the hydrocarbon core and the aqueous medium—that is, the solubilizing power of the core.

Example 15–3. (*a*) Compute the factor χ in reducing the solubility of a new anesthetic that is solubilized in the core of sodium dodecyl

sulfate micelles. The partial molar volume of the anesthetic drug, $\bar{v}$, is 173 cm^3/mole. The micelle–water interfacial tension is 31.3 erg/cm^2, and the radius r of the micelle is 18 Å.

(*b*) If the partition coefficient, dodecane–water, of the drug compound is $K = 21.9$, what is the partition coefficient of the anesthetic solubilizate in the core–water system?

(*a*) First, we compute the Laplace pressure P for the micelles of the surfactant, sodium dodecyl sulfate. Using equation (15–35),

$$P = 2\gamma/r = (2 \times 31.3 \text{ erg/cm}^2)/(18 \times 10^{-8} \text{ cm})$$

$$P = 3.48 \times 10^8 \text{ dyne/cm}^2 \text{ or } 343 \text{ atm}$$

$$(1 \text{ dyne/cm}^2 = 9.869 \times 10^{-7} \text{ atm})$$

Notice how great is the pressure (343 atm) inside the micelle core when its radius is small (r = 18 Å)! From equation (15–36),

$$\ln \chi = \frac{P\bar{v}}{RT} = \frac{(3.48 \times 10^8 \text{ dyne/cm}^2) \times (173 \text{ cm}^3\text{/mole})}{8.3143 \times 10^7 \text{ erg deg}^{-1} \text{ mole}^{-1} \times 298^\circ \text{ K}}$$

$$\ln \chi = 2.43; \chi = 11.36$$

Thus the solubility of the new anesthetic drug in the hydrocarbon core of the surfactant is reduced by a factor of 11.36 relative to its solubility in dodecane, due to the Laplace pressure on the micelle.

(*b*) The partition coefficient of the new compound in the micellar core–water system is obtained by dividing the partition coefficient K in dodecane–water by the χ value obtained in part (*a*):

$$\text{Partition coefficient (core–water)} = 21.9/11.36 = 1.93$$

That is to say, the distribution of the drug compound in the core of the micelle is roughly twice that in the water phase.

The fraction of drug located at the surface of the micelle in the "adsorbed" state is related to the surface activity of the drug. Benzene is moderately surface-active at the heptane–water interface. However, its surface activity is greatly magnified in micellar solution owing to the extremely high surface-to-volume ratio of the micelles. Thus, the surface activity of benzene in micelles provides an explanation of its location mainly at the surface, that is, in the "adsorbed" state.

The pharmacist must give due attention to several factors when attempting to formulate solubilized systems successfully. It is essential that, at the concentration employed, the surface-active agent, if taken internally, be nontoxic, miscible with the solvent (usually water), compatible with the material to be solubilized, free from disagreeable odor and taste, and relatively nonvolatile. Toxicity is of paramount importance, and, for this reason, most solubilized systems are based on nonionic surfactants. The amount of surfactant used is important: a large excess is undesirable, from the point of view of both possible toxicity and reduced absorption and activity; an insufficient amount can lead to precipitation of the solubilized material. The amount of material that can be solubilized by a given amount of surfactant is a function of the polar–nonpolar characteristics of the surfactant (commonly termed the *hydrophile–lipophile balance*, or HLB; see p. 371) and of the molecule being solubilized.

It should be appreciated that changes in absorption and biologic availability and activity may occur when the material is formulated in a solubilized system. Drastic changes in the bactericidal activity of certain compounds take place when they are solubilized, and the pharmacist must ensure that the concentration of surface-active agent present is optimum for that particular system. The stability of materials against oxidation and hydrolysis may be modified by solubilization.

Solubilization has been used in pharmacy to bring into solution a wide range of materials including volatile oils, coal tar and resinous materials, phenobarbital, sulfonamides, vitamins, hormones, and dyes.[27,35]

A new antimalarial drug, β-arteether, isolated in China from the plant *Artemesia annua L.*, is highly active against both chloroquine-sensitive and chloroquine-resistant forms of *Plasmodium falciparum*, the protozoa that spends part of its life cycle in the *Anopheles* mosquito. The drug is very insoluble (17 mg/L) in water but quite soluble (>200 g/L) in various organic solvents. Krishna and Flanagan[36] studied the solubilization of β-arteether in a number of anionic, cationic, and nonionic surfactant solutions above their critical micelle concentrations. They found that anionic and cationic surfactants increased the solubility dramatically by micellar solubilization, while nonionic surfactants showed little effect in enhancing the solubility of the drug. The increase in solubility of β-arteether with increasing micellar concentration of two anionic surfactants and one cationic surfactant is shown in Figure 15–14. On the vertical axis is given the relative solubility of the drug, expressed as S_t/S_o, where S_t is the total solubility of β-arteether in micellar solution and S_o is the solubility of the drug in water alone.

O'Malley et al.[37] investigated the solubilizing action of Tween 20 on peppermint oil in water and presented their results in the form of a tenary diagram as shown in Figure 15–15. They found that on the gradual addition of water to a 50:50 mixture of peppermint oil and Tween 20, polysorbate 20, the system changed from a homogeneous mixture (region I) to a viscous gel

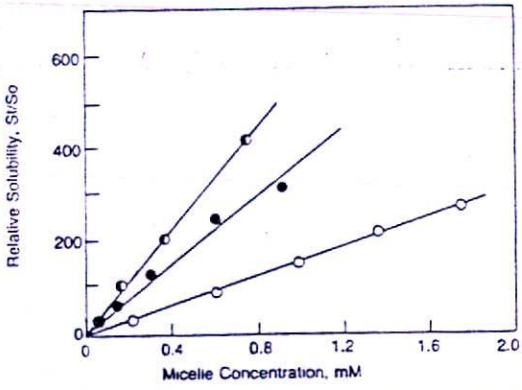

Fig. 15–14. Relative solubility, S_t/S_o, versus micelle concentration of β-arteether. Key: ○ = decyl sodium sulfate; ◐ = tetradecyl sodium sulfate; ● = hexadecyl trimethylammonium bromide. (From A. K. Krishna and D. R. Flanagan, J. Pharm. Sci. 78, 574, 1989, reproduced with permission of the copyright owner.)

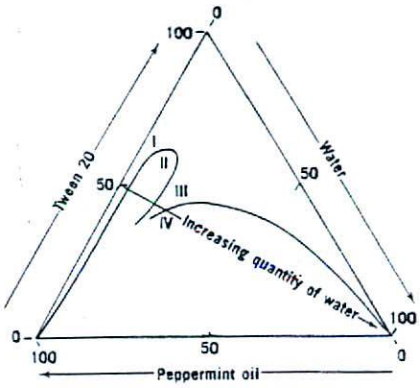

Fig. 15–15. Phase diagram for the ternary system water, Tween 20, and peppermint oil.

(region II). On the further addition of water, a clear solution (region III) again formed, which then separated into two layers (region IV). This sequence of changes corresponds to the results one would obtain by diluting a peppermint oil concentrate in compounding and manufacturing processes. Analyses such as this therefore can provide important clues for the research pharmacist in the formulation of solubilized drug systems.

Determination of a phase diagram was also carried out by Boon and co-workers[38] in order to formulate a clear, single-phase liquid vitamin A preparation containing the minimum quantity of surfactant needed to solubilize the vitamin. Phase equlibrium diagrams are particularly useful when the formulator wishes to predict the effect on the phase equilibria of the system of dilution with one or all of the components in any desired combination or concentration.

Factors Affecting Solubilization. The solubilization capacity of surfactants for drugs varies greatly with the chemistry of the surfactants and with the location of the drug in the micelle. If a hydrophobic drug is solubilized in the micelle core, an increase of the lipophilic alkyl chain length of the surfactant should enhance solubilization. At the same time, an increase in the micellar radius by increasing the alkyl chain length reduces the Laplace pressure, thus favoring the entry of drug molecules into the micelle (see *Example 15–9*).

For micelles consisting of ionic surfactants, an increase in the radius of the hydrocarbon core is the principal method of enhancing solubilization,[39] whereas for micelles built up from nonionic surfactants, evidence of this effect is not well-grounded. Attwood et al.[40] have shown that an increase of carbon atoms above 16 in an *n*-polyoxyethylene glycol monoether—a nonionic surfactant—increases the size of the micelle but, for a number of drugs, does not enhance solubilization. Results from NMR imaging, viscosity and density testing[41] suggested that some of the polar groups of the micelle, that is, some polyoxyethylene groups outside the hydrocarbon core of the micelle, double back and intrude on the core depressing its melting point and producing a fluid micellar core (Fig. 15–16). However, this movement of polyethylene groups into the hydrocarbon core disrupts the palisade layer and tends to destroy the region of solubilization for polar–nonpolar compounds (semipolar drugs).

Patel et al.[42] suggested that the solubilizing nature of the core be increased with a more polar surfactant that would not disrupt the palisade region. Attwood et al.[40] investigated the manner in which an ether or keto group introduced into the hydrophobic region of a surfactant, octadecylpolyoxyethylene glycol monoether, affects the solubilization and micellar character of the surfactant. It was observed that the ether group lowered the melting point of the hydrocarbon and thus was able to create a liquid core without the intrusion phenomenon, which reduced the solubilizing nature of the surfactant for semipolar drugs.

The principal effect of pH on the solubilizing power of nonionic surfactants is to alter the equilbrium between the ionized and un-ionized drug (soiubilizate). This affects the solubility in water (pp. 233–234) and modifies the partitioning of the drug between the micellar and the aqueous phases. As an example, the more lipophilic un-ionized form of benzoic acid is solubilized to a greater extent in polysorbate 80[43] than the more hydrophilic ionized form. However, solubilization of drugs having hydrophobic parts in the molecule and more than one dissociation constant may not correlate with lipophilicity of the drug. Ikeda et al.[44] studied the solubilization of tetracycline by nonionic, anionic, and cationic surfactants. Tetracycline derivatives may exist in solution as positively and/or negatively charged species (zwitterions, p. 149) as a function of pH. At the pH range of 2.1 to 5.6 the species present are the cationic form and the zwitterionic form, and both contribute to the apparent partition coefficient in a micelle–water system. The equilibrium can be represented as[44]

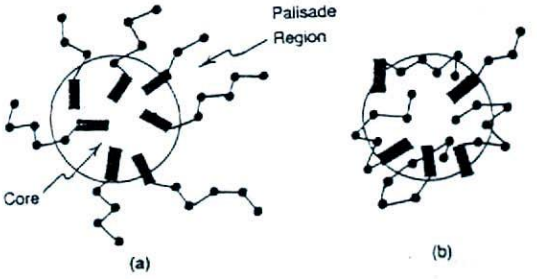

Fig. 15–16. Schematic of nonionic micelle of *n*-polyoxyethylene glycol monoether showing intrusion of polyoxyethylene chains into the micelle core. (*a*) Micelle with palisade environment intact. (*b*) Palisade layer partially destroyed by loss of polyoxyethylene groups into the hydrophobic core.

$$C_m^+ \overset{K_c}{\rightleftharpoons} C_w^+ \overset{K_1}{\rightleftharpoons} C_w^{\pm} \overset{K_z}{\rightleftharpoons} C_m^{\pm}$$

where K_1 is the first dissociation constant of tetracycline derivatives and K_c and K_z are the partition coefficients for the system, micelle–water, for the cationic (+) and zwitterionic (±) species. C_m and C_w denote the drug concentration in the micellar and aqueous phases, respectively. The apparent partition coefficient K_{app} is related to pH as follows[44]:

$$K_{app}([H^+]_w + K_1) = K_c[H^+]_w + K_zK_1 \qquad (15-37)$$

where $[H^+]$ is the hydrogen ion concentration in the aqueous phase. Using this equation, K_c and K_z can be estimated from the slope and the intercept of a linear plot or a regression of $K_{app}([H^+]_w + K_1)$ against $[H^+]_w$.

Example 15–10. The apparent partition coefficient K_{app} (micelle–water) of tetracycline solubilized in micelles of the nonionic surfactant polyoxyethylene lauryl ether, at 25° C and at several pH values, is given in the following table:

pH	2.1	3.0	3.9	5.6
K_{app}	8.05	7.61	6.54	5.68

Compute the partition coefficients of the zwitterionic, K_z, and cationic, K_c, species. The dissociation constant given by Ikeda et al.[44] for tetracycline is $K_1 = 4.68 \times 10^{-4}$.

First, we compute the term $K_{app}([H^+]_w + K_1)$ at the several pH values. For example, at pH = 2.1, $[H^+]_w = 7.943 \times 10^{-3}$ and $K_{app}([H^+]_w + K_1) = 8.05[(7.943 \times 10^{-3}) + (4.68 \times 10^{-4})] = 0.068$. Analogous calculations give the results in the table below, where pH is converted into $[H^+]_w$ concentration:

$[H^+]_w \times 10^3$	7.94	1.00	0.126	0.0025
$K_{app}([H^+]_w + K_1)$	0.068	0.011	0.0039	0.0027

Now we regress $K_{app}([H^+]_w + K_1)$ against $[H^+]_w$ from the values given in the table to obtain the slope, $K_c = 8.21$ and the intercept, $K_1K_z = 2.776 \times 10^{-3}$. Solving for K_z we have

$$K_z = \frac{2.776 \times 10^{-3}}{4.68 \times 10^{-4}} = 5.93$$

The results indicate that the cationic form is more solubilized than the zwitterionic form, that is, $K_c > K_z$. Ikeda et al. suggested that the greater solubilization of the cationic form of tetracycline is due to the formation of hydrogen bonds between an acidic proton of the cationic species of tetracycline and the oxygen atom of the polyoxyethylene chain of the nonionic surfactant. Since the zwitterionic form of tetracycline has lost its acidic proton it cannot hydrogen-bond; thus, it is solubilized to a lesser extent.

Tetracycline is solubilized much more in micelles of an anionic surfactant, sodium lauryl sulfate, than in micelles of cationic surfactants, such as trimethyl ammonium, particularly at pH 2.1. The cationic form of tetracycline predominates at pH 2.1. At this pH value, Ikeda et al.[44] found that $K_{app} = 2860$ in the anionic surfactant. This is due to the greatest interaction occurring at pH 2.1 between the protonated species of the drug and the anionic micelles of sodium lauryl sulfate. On the other hand, the electrostatic repulsion between the cationic form of the drug and dodecyltrimethyl ammonium, the cationic micelle, does not result in solubilization at pH 2.1; thus, at this pH value $K_{app} = 0$. The repulsion is reduced as the pH increases since the cationic nature of the drug decreases. Consequently, solubilization of tetracycline in the cationic surfactant micelles becomes greater with an increase of pH.

Thermodynamics of Solubilization.[45] Solubilization may be considered as a partitioning of the drug between the micellar phase and the aqueous environment. Thus, the standard free energy of solubilization, ΔG_s°, can be computed from the partition coefficient K of the micelle/aqueous medium:

$$\Delta G_s^\circ = -RT \ln K \qquad (15-38)$$

The standard free enthalpy and entropy of solubilization can be computed from the usual relationships:

$$\ln K = \frac{-\Delta H_s^\circ}{R}\frac{1}{T} + \text{constant} \qquad (15-39)$$

and

$$\Delta G_s^\circ = \Delta H_s^\circ - T\Delta S_s^\circ \qquad (15-40)$$

The sign and magnitude of the thermodynamic functions ΔH_s° and ΔS_s° may be related to the location of the solubilized drug in the micelle as follows. The solubilization of a hydrocarbon in the hydrophobic core is similar to hydrocarbon transfer from water to an organic medium. In both cases the thermodynamic functions are of the same order of magnitude. The standard free enthalpy is approximately zero or a small positive number; and ΔG_s° ordinarily is negative. The main contribution to the negative ΔG_s° is a strongly positive entropy change. Due to their hydrophobicity, hydrocarbons dissolve mainly in the core of the micelle.

For a polar solute, ΔG_s° of transfer from an aqueous to an organic medium is positive and ΔS_s° is negative. These unfavorable terms may be associated with poor penetration of the solute into the organic phase. This argument can be applied to the penetration of a polar solute into the core of a micelle. The thermodynamic functions for transfer of various solutes of different polarity from water to micellar solutions and to organic solvents at 25° C are given in Table 15–6. Benzoic acid is considered to be mainly adsorbed on the micellar surface of nonionic surfactants; the thermodynamic functions ΔG_s°, ΔH_s°, and ΔS_s° for benzoic acid solubilization are negative (see Table 15–6). Barbituric acid derivatives solubilized in sodium alkyl sulfonate, an anionic surfactant, show ΔG_s°, ΔH_s°, and ΔS_s° values similar to those of benzoic acid. Barbiturates must be distributed in the most exterior part of the micelle—the polyoxyethylene region—rather than the hydrocar-

TABLE 15–6. *Transfer of Solutes from Water to Organic Solvents or Micelles at 25° C*[45]

Solute	Organic Medium	ΔG° (cal/mole)	ΔH° (cal/mole)	ΔS° [cal/(mole deg)]
Ammonium chloride	Ethanol	−5010	−2830	−26.3
Methane	Cyclohexane	−2280	+2380	−15.6
Amobarbital	Micellar solution*	−2340	−1700	−2.1
Barbital	Micellar solution*	−790	−2600	−6.0
Benzoic acid	Micellar solution†	−2320	−3700	−4.7
Ethane	Micellar solution	−3450	+2000	+18.3
Phenobarbital	Micellar solution*	−1850	−3800	−6.5
Propane	Micellar solution*	−4230	+1000	+17.5

*Sodium lauryl sulfate, 0.06 mole/liter.
†*n*-Alkylpolyoxyethylene, $E_{16}H_{16}$.

bon core owing to their negative ΔS_t° value. These results with benzoic acid and barbiturates can perhaps be explained by the reasoning given in Table 11–11, p. 276, where it is shown that the thermodynamic functions ΔH° and ΔS_o are due to several kinds of interactions. In Table 11–11, donor–acceptor and hydrogen bonding are associated with both negative ΔH° and ΔS°, the large negative ΔH° values overcoming the unfavorable entropy change. Thus, ΔG_t° is negative and the solubilization process is spontaneous.

Example 15–11. The apparent partition coefficients, K, for the transfer of barbital between water and sodium alkyl sulfonate at several temperatures are[46]

Temperature (°C)	25	35	45	55
Partition coefficient, K	3.8	3.5	3.2	2.5

Compute ΔG_t°, ΔH_t°, and ΔS_t°.

From equation (15–39), a regression of ln K against $1/T$ (Kelvin degrees) gives ΔH_t° from the slope. The values needed for the regression are shown as

$1/T \times 10^3$	3.36	3.25	3.14	3.05
ln K	1.335	1.253	1.163	0.916

The equation obtained is $\ln K = 1274.35\ 1/T - 2.91$.

$$\Delta H_t^\circ = (\text{slope}) \times (R) = -(1274.35)(1.9872) = -2.5 \text{ kcal/mole}$$

ΔG_t° is obtained from equation (15–38):

$$\text{at } 25^\circ \text{ C}, \Delta G_t^\circ = -(1.9872)(298)(1.335) = -790.57 \text{ cal/mole}$$

Analogous calculations give $\Delta G_t^\circ = -766.91$, -734.93, and -597.05 cal/mole at 35°, 45°, and 55° C.

The ΔS_t° value is obtained using equation (15–40) at each temperature; at 25° C,

$$\Delta S_t^\circ = \frac{\Delta H_t^\circ - \Delta G_t^\circ}{T} = \frac{-2500 - (-790.57) \text{ cal/mole}}{298^\circ \text{ K}}$$

$$= -5.7 \text{ cal/(mole deg)}$$

ΔS_t° is −5.6, −5.6, and −5.8 cal/(mole deg) at 35°, 45°, and 55° C, respectively. Notice that the constant in equation (15–39) is $\Delta S^\circ/R$ (see equation [11–52]). Therefore, ΔS° can also be obtained from the intercept of the regression line on a plot of ln K versus $1/T$; that is, ΔS_t° = (intercept) × (R) = $(-2.91)(1.9872) = -5.8$ cal/(mole deg), a value very similar to the values obtained by the use of equation (15–40) at several temperatures. The ΔG_t° values obtained are not strongly negative owing to the unfavorable negative value of ΔS_t°. The negative ΔH_t° and ΔS_t° may be related to hydrogen bonding (see Table 11–11) of the barbiturates within the polyoxyethylene palisade of the micelles.

Krafft Point and Cloud Point. Another feature of micelle-forming surfactants is the rapid increase in solubility above a definite temperature, known as the *Krafft point*, K_t. The Krafft point is the temperature at which the solubility of the surfactant equals the cmc. Below K_t, an increase in the concentration of the surface-active agent leads to precipitation rather than micelle formation. The surfactant has a limited solubility, and below the Krafft point, the solubility is insufficient for micellization. As the temperature is elevated, the solubility increases slowly. At the Krafft point, corresponding to the critical micelle concentration, the surfactant crystals melt and are incorporated into the micelles. The micelles are highly soluble; therefore, a rapid increase in solubility occurs with increasing temperature above K_t. Not all surfactants show a rapid increase in solubility above a certain temperature. Only certain ionic and nonionic surface-active agents, for example, have been reported to show a Krafft temperature.[46]

The Krafft point, K_t, can be obtained by plotting the logarithm of molar solubility for a surface active carboxylic acid at several pH values against the inverse of the absolute temperature, as seen in Figure 15–17.[47] For a surfactant solution that has a Krafft point the log solubility–reciprocal temperature profile exhibits a break, that is, a change in slope; the temperature at which the break in the curve occurs at a definite pH is the Krafft point. Actually, a curvature rather than a sharp break occurs in the slope, suggesting that K_t is a temperature range rather than a definite point on the temperature scale. The Krafft point at each pH value is estimated from the intersection of the tangents to the two line segments of different slope shown in Figure 15–17 (see *Problem 15–25* for the calculation of K_t for a surface active benzoic acid derivative at pH 7.0). For ionic surfactants, pH has a definite effect on the Krafft point, as observed in Figure 15–17.

A lower consolute temperature, as discussed on page 41, is also observed for many nonionic, polyoxyethylated surfactants in solution. This temperature, above

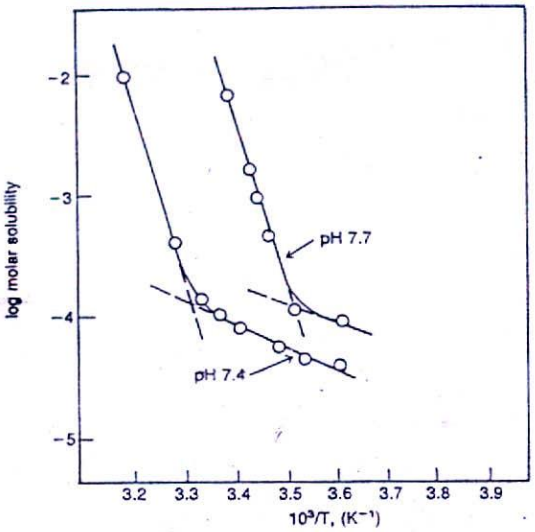

Fig. 15–17. A plot of log solubility against a reciprocal temperature to obtain the Krafft point for a surface-active carboxylic acid at two pH values. (From N. K. Pandit and J. M. Strykowski, J. Pharm. Sci. 78, 768, 1989, reproduced with permission of the copyright owner.)

which cloudiness suddenly appears, is known as the *cloud point*. The surfactant separates as a precipitate, or when in high concentration as a gel, from aqueous solution at an elevated temperature because of self-association and loss of water of hydration of the individual molecules. Schott and Han[46] have reported on the effects of various salts on the Krafft and cloud points of nonionic surfactants, and Schott[48] has compared HLB to the cloud points of a large number of nonionic surfactants.

Coacervation and Cloud Point Phenomena. Solubilization may change certain properties of micelles such as the cloud point and the size of the micelles. Organic solubilizates generally decrease the cloud point of nonionic surfactants. Aliphatic hydrocarbons tend to raise the cloud point, whereas aromatic hydrocarbons and alkanols may lower or raise the cloud point of the surfactant, depending on its concentration. For example, both indomethacin, an antiinflammatory drug, and sorbitol lower the cloud point of 2% aqueous solutions of the nonionic surfactant polysorbate 80. The effect is more pronounced for sorbitol and increases linearly with sorbitol concentration.[49] Indomethacin, a drug of very low aqueous solubility, can be considered to be entirely located within the micellar phase of polysorbate 80 in aqueous solution. Solubilized indomethacin increases the micellar size due not only to incorporation of drug molecules in the polysorbate micelles but also to an increase in the number of polysorbate monomers per micelle, that is, the *aggregation number*. The increase in micellar size suggests a restructuring of the micelle to accommodate the indomethacin molecules, the larger size producing a more symmetrical micelle with greater hydration.

That solubilizates may favor the transition from rodlike to globular micelles has been recently investigated.[50] Rod-shaped micelles are found in nonionic as well as ionic surfactant solutions in which the charge on the micelle is shielded by salt ions or by strongly binding counterions. The solubilizing capacity of these systems is particularly large when near to coacervate formation. An example is the phase separation of nonionic surfactants above the cloud point. The long rods are transformed into globular micelles after a certain amount of aliphatic or aromatic hydrocarbon is solubilized. The difference between the solubilization of aliphatic and aromatic hydrocarbons by rod-shaped micelles is that the aromatic compounds can lead to coacervate formation before the aggregates shrink and are transformed into spherical micelles. This process is explained as follows. After solubilization of the aromatic hydrocarbon by rodlike aggregates the system separates into two phases with formation of a coacervate. Coacervation can be described as a transition from a solution with rodlike micelles in the gaseous state into two solutions, one of which is in a more condensed state and the other in a more dilute state. The condensed micellar aggregates can still accommodate more hydrocarbon; and after further addition of hydrocarbon the transition from rods to globules takes place. The attractive forces between the small globules are weak and the system cannot simultaneously be in a condensed and a gaseous state. It reverts back to the isotropic single-phase state. Thus, these systems show the interesting phenomenon that a two-phase binary surfactant system (a coacervate) can be transformed into a single-phase solution by solubilization of hydrocarbons[50] in the micelles.

The fact that rodlike micelles can be changed into globular micelles has considerable interest in the practical application of surfactants. Surfactant systems with rodlike micelles may have high viscosities. If highly viscous systems are not desired, one can solubilize enough hydrocarbon to break the rods. When the long rods are transformed into globular micelles the attractive forces between the micelles become smaller and the cloud point of nonionic surfactants is increased. That is, the solubility of the surfactant in the medium becomes greater. Thus, rod–sphere transitions provide an explanation for the rather unusual increase of the cloud point by solubilization of hydrocarbons in the micelles. Alcohols stabilize the rods and for this reason lower the cloud point.[50] That is to say, alcohols decrease the solubility of the surfactant.

ADDENDUM: THERMODYNAMICS OF MICELLIZATION

Two models can be used to explain the properties of micellar solutions.[51] According to the *phase-separation*

model, micellization can be considered as the formation of a separate phase in a bulk aqueous medium. Below the cmc, the system contains surfactant molecules (monomers) molecularly dispersed in water. Above the cmc, the system contains two phases in equilibrium: one consisting of monomers of the surfactant in aqueous solution and the other represented by micelles of the surfactant. In this model, micellization is not a progressive association of the surfactant monomer but rather a one-step process.[52]

The second approach is provided by the *mass-action model*. According to this view, micellization can be considered as a stepwise association of monomers to form an aggregate. This model is appropriate when micelles are relatively small. Thoma and Christian[51] have shown that the phase-separation model is a special case of the mass-action model when the aggregation number of the micelles is large. (The *aggregation number* is simply the number of surfactant molecules that come together to form a single micelle.) Both models can be combined to derive an expression for the *standard free energy micellization*.

In the formation of an ionic micelle from an anionic surfactant, such as sodium lauryl sulfate ($C_{12}H_{25}SO_4^-Na^+$, abbreviated R^-X^+) n amphiphilic ions R^-, together with m counterions X^+, form a negatively charged micelle:

$$nR^- + mX^+ \rightleftharpoons [R_nX_m]^{Q-} \qquad (15\text{–A1})$$

where Q^- is the net charge on the micelle, $Q^- = n - m$, n is the aggregation number, and m is the number of counterions bound to the micelle (see Fig. 15–18). For example, for a micelle of $C_{12}H_{25}SO_4^-Na^+$, the aggregation number[53] $n = 50$ ($C_{12}H_{25}SO_4^-$), or 50 negatively charged lauryl sulfate ions, and $m = 45$ Na^+, or 45 positively charged sodium ions. Therefore, the charge on the micelle is $Q = n - m = 5$ negative charges.

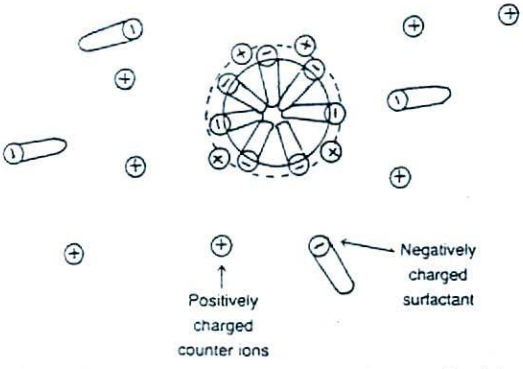

Fig. 15–18. Schematic of an anionic micelle where $n = 7$ and the charge $Q = 7 - 4 = 3^-$. The four positive ions needed for electroneutrality are immediately outside the micelle. The figure shows monomers of the dissociated surfactant in equilibrium with the micelle, as expressed in equation (15–A1). A more realistic example is given in the text where $n = 58$.

To give electroneutrality, five positively charged Na^+ ions must also be present in solution in the outside palisade region of the micelle; they are not considered in equation (15–A1). From the mass-action law, the equilibrium constant is

$$K = \frac{[R_nX_m]^{Q-}}{[R^-]^n[X^+]^m} \qquad (15\text{–A2})$$

or, as for the example above,

$$K = \frac{[(C_{12}H_{25}SO_4^-)_{50}\,(Na^+)_{45}]^5}{[C_{12}H_{25}SO_4^-]^{50} \cdot [Na^+]^{45}} \qquad (15\text{–A3})$$

The standard free energy of micellization, ΔG°_{mic}, that is, the standard free energy per mole of surfactant monomer, $\Delta G^\circ/n$, is

$$\Delta G^\circ_{mic} = \frac{\Delta G^\circ}{n} = -\frac{RT}{n} \ln K \qquad (15\text{–A4})$$

Notice that each term is divided by the aggregation number n to give the *free energy per individual monomer*. From equations (15–A3) and (15–A4),

$$\Delta G^\circ_{mic} = -\frac{RT}{n} \ln \frac{[R_nX_m]^{Q-}}{[R^-]^n[X^+]^m} \qquad (15\text{–A5})$$

According to the phase-separation model, at the cmc the concentration of monomers is $[R^-] = [X^+] = \text{cmc}$. Rearranging equation (15–A5), we have

$$\Delta G^\circ_{mic} = -RT\left[\frac{1}{n} \ln [R_nX_m]^{Q-} - \ln (\text{cmc}) - \frac{m}{n} \ln (\text{cmc})\right] \qquad (15\text{–A6})$$

At the cmc, the term $1/n \ln [R_nX_m]^{Q-}$ may be neglected.[54] Thus, equation (15–A6) reduces to

$$\Delta G^\circ_{mic} = RT\left(1 + \frac{m}{n}\right) \ln (\text{cmc}) \qquad (15\text{–A7})$$

or, since $m = n - Q^-$, equation (15–A7) can also be written

$$\Delta G^\circ_{mic} = RT\left(2 - \frac{Q^-}{n}\right) \ln (\text{cmc}) \qquad (15\text{–A8})$$

Knowing the cmc, the aggregation number n, and the charge on the micelle, one can calculate ΔG°_{mic} for an anionic micelle. The same equation can be applied to a cationic micelle, substituting Q^- in equation (15–A8) with the positive charge Q^+ on the micelle (see Problem 15–29). Q^+ and Q^- are determined from the degree of ionization (p. 130) of the surfactant, which in turn is obtained by light scattering, EMF, or conductivity measurements.

For nonionic micelles, $m = 0$ and equation (15–A8) becomes

$$\Delta G^\circ_{mic} = RT \ln (\text{cmc}) \qquad (15\text{–A9})$$

The standard enthalpy and entropy changes of micellization can be computed from the expressions

$$\ln (\text{cmc}) = -\frac{\Delta H^\circ_{\text{mic}}}{R}\frac{1}{T} + \frac{\Delta S^\circ_{\text{mic}}}{R} \quad (15\text{-A10})$$

and

$$\Delta G^\circ_{\text{mic}} = \Delta H^\circ_{\text{mic}} - T\Delta S^\circ_{\text{mic}} \quad (15\text{-A11})$$

The standard free energy for a nonionic micelle is calculted in Problem 15–31.

References and Notes

1. H. K. Chan and I. Gonda, J. Pharm. Sci. 78, 176, 1989.
2. C. J. Drummond, G. G. Warr, F. Grieser, B. W. Nihaen and D. F. Evans, J. Phys. Chem. 89, 2103, 1985.
3. Y. Chang and J. R. Cardinal, J. Pharm Sci. 67, 994, 1978.
4. T. J. Racey, P. Rochon, D. V. C. Awang and G. A. Neville, J. Pharm. Sci. 76, 314, 1987; T. J. Racey, P. Rochon, F. Mori and G. A. Neville, J. Pharm. Sci. 78, 214, 1989.
5. P. Mukerjee, J. Phys. Chem. 76, 565, 1972.
6. K. W. Herrmann, J. Colloid Interface Sci. 22, 352, 1966.
7. P. C. Hiemenz, *Principles of Colloid and Surface Chemistry*, 2nd. Edition, Dekker, New York, 1986, pp. 127, 133, 148.
8. J. Kirschbaum, J. Pharm. Sci. 63, 981, 1974.
9. A. J. Richard, J. Pharm. Sci. 64, 873, 1975.
10. H. Arwidsson and M. Nicklasson, Int. J. Pharm. 58, 73, 1990.
11. H. H. Paradies, Eur. J. Biochem. 118, 187, 1981.
12. H. H. Paradies, J. Pharm. Sci. 78, 230, 1989.
13. H. Schott, J. Pharm. Sci. 70, 486, 1981.
14. H. Takenaka, Y. Kawashima and S. Y. Lin, J. Pharm. Sci. 70, 302, 1981.
15. D. J. A. Crommelin, J. Pharm. Sci. 73, 1559, 1984.
16. H. Schott and C. Y. Young, J. Pharm. Sci. 61, 182, 1972.
17. H. Schott and E. Astigarrabia, J. Pharm. Sci. 77, 918, 1988.
18. T. Higuchi, R. Kuramoto, L. Kennon, T. L. Flanagan and A. Polk, J. Am. Pharm. Assoc., Sci. Ed. 43, 646, 1954.
19. E. J. W. Verwey and J. Th. G. Overbeek, *Theory of the Stability of Lyophobic Colloids*, Elsevier, Amsterdam, 1948.
20. B. Derjaguin and L. Landau, Acta Physica. Chim., USSR, 14, 663, 1941; J. Exp. Theor. Physics, USSR, 11, 802, 1941.
21. H. Takenaka, Y. Kawashima and S. Y. Lin, J. Pharm. Sci. 69, 513, 1980.
22. A. A. Badawi and A. A. El-Sayed, J. Pharm. Sci. 69, 492, 1980.
23. H. Schott, in *Remington's Pharmaceutical Sciences*, 16th Edition, Mack Publishing, Easton, Pa., 1980, Chapter 20.
24. E. Haines and A. N. Martin, J. Pharm. Sci. 50, 228, 753, 756, 1961.
25. B. A. Mulley, in *Advances in Pharmaceutical Sciences*, Academic Press, New York, 1964, Vol. 1, pp. 87–194.
26. T. Nakagawa, in *Nonionic Surfactants*, M. J. Schick, Dekker, New York, 1967.
27. P. H. Elworthy, A. T. Florence and C. B. Macfarlane, *Solubilization by Surface-Active Agents*, Chapman & Hall, London, 1968.
28. D. Attwood and A. T. Florence, *Surfactant Systems*, Chapman & Hall, London and New York, 1983.
29. C. Engler and E. Dieckhoff, Arch. Pharm. 230, 561, 1892.
30. A. S. C. Lawrence, Trans. Faraday Soc. 33, 815, 1937.
31. E. Keh, S. Partyka and S. Zaini, J. Colloid Interface Sci. 129, 362, 1989.
32. I. Reich, J. Phys. Chem. 60, 260, 1956.
33. P. Mukerjee and J. Cardinal, J. Phys. Chem. 82, 1620, 1978.
34. C. Ramachandran, R. A. Pyter and P. Mukerjee, J. Phys. Chem. 86, 3198, 1982.
35. B. W. Barry and D. I. El Eini, J. Pharm. Pharmacol. 28, 210, 1976.
36. A. K. Krishna and D. R. Flanagan, J. Pharm. Sci. 78, 574, 1989.
37. W. J. O'Malley, L. Pennati and A. Martin, J. Am. Pharm. Assoc., Sci. Ed. 47, 334, 1958.
38. P. F. G. Boon, C. L. J. Coles and M. Tait, J. Pharm. Pharmacol. 13, 200T, 1961.
39. T. Anarson and P. H. Elworthy, J. Pharm. Pharmacol. 32, 381, 1980.
40. D. Attwood, P. H. Elworthy and M. J. Lawrence, J. Pharm. Pharmacol. 41, 585, 1989.
41. P. H. Elworthy and M. S. Patel, J. Pharm. Pharmacol. 36, 565; ibid. 36, 116, 1984.
42. M. S. Patel, P. H. Elworthy and A. K. Dewsnup, ibid, 33, 64P, 1981.
43. J. H. Collett and L. Koo, J. Pharm. Sci. 64, 1253, 1975.
44. K. Ikeda, H. Tomida and T. Yotsuyanagi, Chem. Pharm. Bull. 25, 1067, 1977.
45. V. Vaution, C. Treiner, F. Puisieux and J. T. Carstensen, J. Pharm. Sci. 70, 1238, 1981.
46. H. Schott and S. K. Han, J. Pharm. Sci. 65, 979, 1976; ibid. 66, 165, 1977.
47. N. K. Pandit and J. M. Strykowski, J. Pharm. Sci. 78, 767, 1989.
48. H. Schott, J. Pharm. Sci. 58, 1443, 1969.
49. D. Attwood, G. Ktistis, Y. McCormick and M. J. Story, J. Pharm. Pharmacol. 41, 83, 1989.
50. H. Hoffmann and W. Ulbricht, J. Colloid Interface Sci. 129, 388, 1989.
51. D. C. Thomas and S. D. Christian, J. Colloid Interface Sci. 78, 466, 1980.
52. W. Binana-Limbele and R. Zana, Colloid Polymer Sci. 267 440, 1989.
53. D. Attwood and A. T. Florence, *Surfactant Systems*, Chapman & Hall, London and New York, 1983, p. 93.
54. P. C. Hiemenz, *Principles of Colloid and Surface Chemistry*, 2nd Edition, Dekker, New York, 1986, pp. 441–448.
55. D. Attwood and O. K. Udeala, J. Pharm. Pharmacol. 26, 854, 1974.
56. H. V. Tartar and A. L. M. Lelong, J. Phys. Chem. 59, 1185, 1956.
57. A. Einstein, *Investigations on the Theory of Brownian Movement*, Dover, New York, 1956.
58. D. J. Shaw, *Introduction to Colloid and Surface Chemistry*, Butterworths, Boston, 1970, pp. 20, 21.
59. L. J. Ravin, E. G. Shami and E. S. Rattie, J. Pharm. Sci. 64, 1830, 1975.
60. S. Chibowski, J. Colloid Interface Sci. 134, 1, 174, 1990.
61. H. Schott, J. Pharm. Sci. 65, 855, 1976.
62. K. A. Johnson, G. B. Westermann-Clark and D. O. Shah, J. Colloid Interface Sci. 130, 480, 1989.
63. M. J. Rosen et al., J. Phys. Chem. 86, 541, 1982; ibid., Colloids Surf. 3, 201, 1981.

Problems

15–1. The equivalent conductivity Λ of a solution containing a surface active agent decreases sharply at the critical micelle concentration owing to the lower mobility of micelles. A plot of Λ (vertical axis) against the concentration or the square root of the concentration of the surface active agent shows an inflection point at the critical micelle concentration. (See Figure 15–3)

Chlorcyclizine hydrochloride, an antihistamine used for the

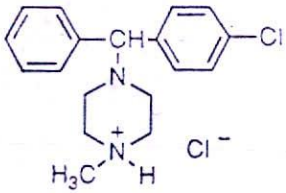

Chlorcyclizine Hydrochloride

relief of urticaria and hay fever, is surface active and forms micelles in aqueous solution. The dependence of Λ in mho m^2 $mole^{-1}$ (see p. 127 for the unit, mho) on $\sqrt{c}$ is given below (partially based on the data of Attwood and Udeala[55]):

Data for Problem 15–1

$\Lambda \times 10^3$ mho m^2 $mole^{-1}$	4.7	5.1	6.0	6.6	7.0	7.5	8.0	8.7
$\sqrt{c}$ (mole/liter)$^{1/2}$	0.33	0.30	0.26	0.24	0.23	0.20	0.17	0.14

Plot Λ versus $\sqrt{c}$ and estimate the cmc.

Answer: cmc = 0.053 mole/liter

15–2. The turbidity τ of an aqueous sodium dodecylbenzene sulfonate (SDBS) solution was determined in a light-scattering photometer at various concentrations above its cmc (modified from data in Tartar and Lelong[56]).

Data for Problem 15–2

$c \times 10^3$ (g/cm^3)	2.68	7.58	13.30	22.15
$\tau \times 10^4$ (cm^{-1})	1.09	1.80	2.08	2.31

The turbidity τ increases with concentration because the surfactant molecules aggregate to form structures with molecular weights much greater than the molecular weight of the monomer SDBS, namely, 349 g/mole. The value of H in equation (15–2), page 399, is 4.00×10^{-6} mole cm^2 g^{-2}. Plot Hc/τ versus c and using equation (15–2) obtain the molecular weight of the aggregate in the aqueous solution. Also give the value of the solute–solvent interaction constant B. The degree of aggregation is obtained by dividing the molecular weight of the aggregate by the molecular weight of the SDBS monomer. What is the degree of aggregation?

Answer: M = 17,170 g/mole; slope = $2B$ = 0.0147; $B = 7.35 \times 10^{-3}$ mole cm^3 g^{-2}. Degree of aggregation = 49, that is, each micelle contains an average of 49 molecules of SDBS.

15–3. The average displacement, $\bar{x}$ in meters, of a microscopic particle is related to its diffusion D (m^2/sec) and the time t of movement. The relation according to Einstein[57] is $\bar{x} = \sqrt{2Dt}$. If a particle moves in a fluid medium with a diffusion coefficient of $D = 2.72 \times 10^{-10}$ meter^2/sec, what is its average Brownian displacement over a time interval of 2.20 sec?

Answer: $\bar{x} = 3.54 \times 10^{-5}$ meter = 3.54×10^{-3} cm.

15–4. For spherical particles we may express the diffusion in terms of their radii r, the viscosity η of the medium, and the absolute temperature T (equation (15–7), p. 401). In 1908 Perrin used this equation and a suspension of gamboge particles of accurately determined size to calculate Avogadro's constant N_A. He obtained values lying between 5.5×10^{23} particles/mole and 8×10^{23} particles/mole. Currently[58] the accepted value of N_A is 6.022×10^{23} mole^{-1}.

Using equation (15–7) in the expression $\bar{x} = \sqrt{2Dt}$ we obtain an equation, $\bar{x} = \sqrt{\dfrac{RTt}{3\pi\eta r N_A}}$, for the calculation of the mean Brownian displacement of a particle.

For a particle of radius $r = 10^{-6}$ meter (10^{-4} cm) in water (η = 0.01 poise) at a temperature of 20° C, T = 293.15° K, its displacement $\bar{x}$ is to be observed over a period of 1 hour (t = 3600 sec). R is the gas constant, expressed in units of 8.3143×10^7 erg deg^{-1} mole^{-1}. The poise is expressed as dyne sec/cm^2 or erg sec/cm^3. Calculate the mean Brownian displacement to be expected. How might you use this equation to determine Avogadro's number?

Answer: $\bar{x} = 3.93 \times 10^{-3}$ cm = 39.3 μm or 3.93×10^{-5} meter displacement in 1 hour.

15–5. When insulin solutions are stored at room temperature, a process of self-association occurs and the molecules aggregate. The degree of aggregation is affected by pH, ionic strength, and temperature. The aggregation process was studied in the temperature range of room temperature (20° C) to human body temperature (~35° C) at pH 7.5 and ionic strength μ = 0.1. The diffusion coefficients of aggregates at the various temperatures and viscosities of the solvent are found at the top of the next column.

Compute the hydrodynamic radii of the aggregates at the various temperatures. See the Stokes–Einstein equation. The poise is equal to 1 g cm^{-1} sec^{-1}

Answer: equation (15–7) may be used. It gives 28.4, 54.5, 78.9, and 104 Å at the four temperatures.

Data for Problem 15–5*

T (°C)	20	25	30	35
$D \times 10^7$ (cm^2 sec^{-1})	7.8	4.6	3.7	3.0
η (poises)	0.0097	0.0087	0.0076	0.0072

*Data from H. B. Bohidar, Colloid Polym. Sci. 267, 159, 1989.

15–6. A sample of horse albumin in an aqueous solution at a concentration of c_g = 3.20 grams per liter was placed in an osmometer at 28° C. Its osmotic pressure π was measured and found to be 0.00112 atm. What is the molecular weight of the serum albumin, assuming the solution is sufficiently dilute for the use of equation (15–11)? The gas constant R = 0.0821 liter atm/mole deg.

Answer: 70,641 gram/mole

15–7. The osmotic pressure π of a fraction of polystyrene was determined at 25° C at various concentrations c_g as recorded here:

Data for Problem 15–7

$\pi/c_g \times 10^6$ (1 atm g^{-1})	12.5	16.3	20.0	23.8
c_g (g/liter)	6.0	12	18	24

Calculate the molecular weight and the second virial coefficient, B, for the polystyrene fraction. Use equation (15–13) disregarding the $C \times c_g^2$ and higher terms. Can this large molecular weight be determined by the osmotic pressure method? What other methods are available to obtain the molecular weight of such a large molecule?

Answer: $M = 2.797 \times 10^5$ or 279,700 daltons; $B = 2.56 \times 10^{-7}$ liter mole g^{-2}.

15–8. An ultracentrifuge is operated at 6000 rpm. The mid-point of the cell with the sample in place is 1.2 cm from the center of the rotor. What is the angular acceleration and the number of "g's" acting on the sample?

Answer: Angular acceleration = 4.737×10^5 rad/sec^2, and the number of "g's" is 483 or a force 483 times that of gravity acting on the sample.

15–9. What is the angular velocity ω of an ultracentrifuge such that a micelle moves from a position in the centrifuge cell of x_1 = 5.957 cm to x_2 = 6.026 cm in 15 minutes? (15 × 60 sec per min = 900 sec.) The sedimentation coefficient s is 7.756×10^{-13} sec.[59] Express the result in rpm.

Answer: 38,787 rpm. More realistically it is rounded to 38,800 rpm.

15–10. Find the angular acceleration in rad/sec^2 for an ultracentrifuge with a rotor of radius 6.5 cm rotating at 1200 rpm. Convert this angular acceleration into "g's," assuming that the acceleration due to gravity is 981 cm/sec^2.

Answer: 10.26×10^4 rad/sec^2, or 105 "g's"

15–11. Determine the molecular weight of egg albumin from the following ultracentrifuge data obtained at 20° C: the Svedberg constant, $s = 3.6 \times 10^{-13}$ sec, $D = 7.8 \times 10^{-7}$ cm^2/sec, the partial specific volume, $\bar{v}$ = 0.75 cm^3/g, and the density of water at 20° C is 0.998 g/cm^3.

Answer: 44,727 g/mole ≅ 45,000 g/mole

15–12. The sedimentation coefficient s at 20° C of saramycetin, an antifungal antibiotic, is 5.3 svedberg (1 svedberg = 10^{-13} sec), the diffusion coefficient is $D = 6 \times 10^{-7}$ cm^2 sec^{-1}, and the partial specific volume is $\bar{v}$ = 0.807 cm^3 g^{-1} ($\bar{v}$ is obtained by use of an accurate pycnometer and a microbalance) (selected data from Kirschbaum[8]).

(a) Compute the molecular weight of saramycetin. The density of the solvent is 0.998 g/cm^3.

(b) Compute the radius of the saramycetin particle. Assume that the particles are spherical. The viscosity of the solvent is 1.002×10^{-2} poise.

Answers: (a) 54,613 or 54,600 dalton; (b) radius, r = 36. Å

15–13. Compute the molecular weight of a cellulose nitrate fraction using equation (15–24) where $K = 4.0 \times 10^{-4}$ and $a = 0.990$ at 27° C. The intrinsic viscosity of the fraction is 2.40 $cm^3\ g^{-1}$.

Answer: 67,053 g/mole or 67,000 dalton

15–14. (a) Use the Mark–Houwink expression, equation (15–24), to calculate the intrinsic viscosity $[\eta]$ in dL/g of a methylcellulose polymer having a number average molecular weight of 15,200 g/mole. The constant K is equal to 1.1×10^{-3} dL mole g^{-1}, where dL stands for deciliters, which equals 100 cm^3. The exponent, a, of equation (15–24) is 0.983 and is dimensionless.

(b) The units of dL mole g^{-2} on K are not quite correct in the problem. Can you suggest the exact units?

Answers: (a) 14.2 dL/g; (b) dL $mole^{0.983}$ $gram^{-1.983}$. These units would differ, however, for each polymer having a different a value. Since the Mark–Houwink equation is an empiric one, in practice, the units on K are obtained disregarding altogether the M^a units. The units on K then become the same as those on intrinsic viscosity, dL/g.

15–15. The variation of reduced viscosity η_{sp}/c with concentration for a new nonionic surfactant is given in the table below.

Data for Problem 15–15*

η_{sp}/c	8.96	9.39	9.82	10.25	10.69
c (mole/kg)	0.005	0.01	0.015	0.02	0.025

*Data from D. Attwood, P. H. Elworthy and M. J. Lawrence, J. Pharm. Pharmacol. 41, 585, 1989.

Compute the intrinsic viscosity, $[\eta]$, of the surfactant.

Answer: $[\eta] = 8.53$ kg/mole of solvent = 8.53 $molality^{-1}$

15–16. It requires 40 seconds for a volume of water, density 1.0 g/cm^3, to flow through a capillary viscometer and 614 seconds for an equal volume of a glycerin solution having a density of 1.12 g/cm^3. What is the viscosity at 25° C and the relative viscosity of this solution? The viscosity of water at 25° C is 0.01 poise or 1.0 cp. See pages 454–455 and 461–462.

Answer: Viscosity of the solution is 0.172 poise. Relative viscosity $\eta_1/\eta_2 = 17.2$ (dimensionless).

15–17. The molecular weight of a spherical protein is 20,000 g/mole and the partial specific volume $\bar{v}$ is 0.80 cm^3/g at 20° C. The viscosity of the solvent is 0.01 poise. Calculate the value of D, the diffusion coefficient at this temperature. (See equation (15–8).) Notice that one is dealing with a *cube* root.

Answer: $D = 11.15 \times 10^{-7}$ cm^2/sec

15–18. Polyvinyl alcohol was separated into four fractions of various molecular weights by means of a column packed with the chromatographic gel, Sephadex G-150. Compute the molecular weight of these fractions from the intrinsic viscosities using the Mark–Houwink equation. The value of a is 0.71 (dimensionless) and K is 2.7×10^{-4} $cm^3\ g^{-1}$. The experimental intrinsic viscosities are 0.463, 0.875, 1.09, and 1.15 cm^3/g.[60]

Answer: 36,000, 88,000, 120,000, and 129,000 g/mole

15–19. The intrinsic viscosities $[\eta]$ of several molecular weight fractions M of a new cellulose plasma extender were obtained by plotting η_{sp}/c for each fraction versus the concentration c in g/dL (where 1 dL = 100 cm^3) as seen in Figure 15–9. The resulting intrinsic viscosities, together with the molecular weights M determined separately by osmotic pressure (equation (15–12)) at 25° C, are given as:

Data for Problem 15–19

M (g/mole)	67,820	153,756	206,200	329,150
$[\eta]$ (dL/g)	1.21	2.65	3.54	5.56

(a) Plot $\ln[\eta]$ as the dependent variable versus $\ln M$ (M = molecular weight) to obtain the constants K and a of the Mark–Houwink equation.

(b) Use the values of K and a in the Mark–Houwink expression (equation (15–24)) to calculate the molecular weight of a newly synthesized cellulose plasma extender, the experimentally determined intrinsic viscosity of which is 7.83 dL/g.

Answers: $K = 2.60 \times 10^{-5}$ dL g^{-1}, $a = 0.966$. Using the Mark–Houwink equation in logarithmic form, the molecular weight of the newly synthesized sample is found to be 469,583, or 470,000 daltons.

15–20. The mobility v/E of a silver iodide sol at 20° C in a Burton electrophoresis cell was observed to be 25×10^{-5} cm^2 $volt^{-1}$ sec^{-1}. Compute the zeta potential of the colloid.

Answer: $\zeta = 35.3$ millivolts

15–21. The zeta potential ζ for a colloidal system in an aqueous electrolyte solution is given by the formula

$$\zeta = \frac{4\pi\eta}{\epsilon}\frac{v}{E}(9 \times 10^4)$$

where 9×10^4 converts electrostatic units into volts.

(a) The term $\frac{4\pi\eta}{\epsilon}(9 \times 10^4)$ is given on page 406 as equal approximately to 128 at 25° C and 141 at 20° C. Refer to a handbook of chemistry and physics for the viscosity in poise (dyne sec/cm^2) or g/(cm sec) and the dielectric constant ϵ at 20° C and 25° C and verify the values 128 and 141 for this term in equation (15–28).

(b) The electrophoretic mobility, v/E (in cm/sec per volt/cm) for bentonite in water is given by Schott[61] as $-3.39\ (\pm 0.07) \times 10^{-4}$ at 24° C. The quantity ± 0.07 in parentheses indicates that the value -3.39 was measured experimentally to within a precision of $-3.39 - 0.07 \times 10^{-4}$ to $-3.39 + 0.07 \times 10^{-4}$. The electrophoretic mobility of bismuth subnitrate particles (13.18% w/w) in water at 24° to 25° C is $+2.20\ (\pm 0.09) \times 10^{-4}$ cm/sec per volt/cm. Calculate the zeta potential of bentonite and of bismuth subnitrate at 25° C. Why do we find both positive and negative zeta potential values in this problem?

Partial Answer: Bentonite, $\zeta = -43.4$ millivolts; bismuth subnitrate, $\zeta = +28.2$ millivolts. The reader should see the paper by Schott for the reason for the positive and negative ζ values.

15–22. Compute the ratio of concentrations at equilibrium of diffusible benzylpenicillin ions *outside* to those *inside* a semipermeable membrane when the concentration of an anionic polyelectrolyte inside the sac is 12.5×10^{-3} gram equivalent per liter and that of benzylpenicillin inside the sac is 3.20×10^{-3} mole/liter at equilibrium. Set up the Donnan membrane equilibrium (see equation (15–34)) and solve the equation for the ratio of diffusible benzylpenicillin ions outside to those inside the membrane.

Answer: 2.22 to 1

15–23. The Donnan effect is important in concentrating ions in various body fluid compartments. The interstitial fluid of the body lies between the vascular system with its plasma and erythrocytes and the tissue cells of the body. The plasma and the cells contain nondiffusible protein anions, whereas the interstitial fluid contains only diffusible ions such as K^+, Na^+, and Cl^-. Therefore the Donnan membrane effect in the body is to influence the distribution of the diffusible ions. The protein anions tend to attract and retain small cations (K^+ and Na^+) in the tissue cells and blood vessels, and repel small anions (Cl^-) into the surrounding interstitial fluid.

In the normal body the concentration of plasma protein is 16 mEq liter and that of the chloride ions is 113 mEq/liter. What is the ratio of chloride ions across the interstitial ($\text{fluid}_{\text{outside}}$ – $\text{plasma}_{\text{inside}}$) membrane? *Hint:* The Donnan membrane principle (equation (15–33)) is used to calculate the ratio of chloride ions.

Answer: $[Cl^-]_o/[Cl^-]_i = 1.07$ to 1

15–24. The diffusion of a drug compound, solubilized in a micelle and hindered by passage through microporous membranes, provides a method to control the release of the drug.

The ratio of the diffusion coefficient of a spherical particle in a cylindrical pore (D_p) relative to the diffusion coefficient of the same particle in free solution (D) is given by the following equation[62]:

$$D_p/D = (1 - \xi)^2[1 - 2.1044\,\xi^2 + 2.089\,\xi^3 - 0.948\xi^5] \qquad (15\text{–}41)$$

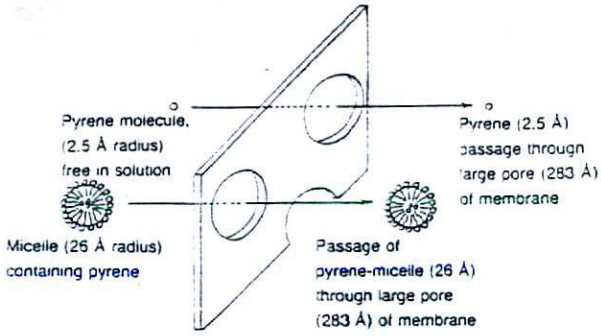

Fig. 15–19. Passage of pyrene, both free in solution and enclosed in a micelle, through large pores of a membrane.

where ξ is rr_p, the ratio of the particle-to-pore radii, and D_p is the intrapore diffusion coefficient. When the radius of the particle is much smaller than the radius of the pore, the intrapore diffusion coefficient is practically the same as the diffusion coefficient in free solution.

The diffusion of pyrene, solubilized in micelles of the surfactant sodium dodecyl sulfate, across microporous membranes at 25° C was studied by Johnson et al.[62] The radius of the micelle is 26 Å and the viscosity of the solvent 0.089 poise. The pore radius of the membrane is 283 Å.

(a) Compute the diffusion coefficient D of the micelle in the free solution (see equation (15–7), p. 401).

(b) Compute the diffusion coefficient, D_p, of the micelle particle in the pore. Compare this value to the diffusion coefficient of free pyrene (not present in micellar form), which is determined in a separate experiment, $D_{free} = 5.6 \times 10^{-6}$ cm²/sec. The radius of the pyrene molecule is approximately 2.5 Å.

(c) Comment on your results. Figure 15–19 is helpful in viewing the problem more clearly.

Answers: (a) $D = 9.4 \times 10^{-8}$ cm²/sec; (b) $D_p = 7.6 \times 10^{-8}$ cm²/sec; (c) *Hint:* Is the radius of the pyrene "particle" larger in the micelle or in free solution? Are the diffusion coefficients directly or inversely proportional to the radii? How can this information be used to design a drug for passage through the membrane pores of a new dosage form?

15–25. The change in molar solubility S with temperature of a surface active carboxylic acid, 3-(4-heptobenzyl) benzoic acid (HBB), in aqueous solution at pH 7.0 is given in the table below (data read from Figure 2 of Pandit and Strykowski[17]).

Plot log S (vertical axis) against $1/T$ (see Fig. 15–17) and estimate the Krafft point K_r of the surfactant. See page 415 for an understanding of the Krafft point.

Answer: $K_r = 43.5°$ C

15–26. According to Pandit and Strykowski[17] the Krafft point can be estimated from a plot of the surface pressure π of saturated solutions of the surfactant as a function of temperature (°C). The surface pressure π is the difference between the surface tensions of the solvent and solution at a fixed temperature, $\pi = \gamma_{solvent} - \gamma_{solution}$. The surface pressure increases with temperature usually because the concentration of surfactant in the saturated solution (the solubility) also increases with temperature. When the Krafft point is reached, any further increase in temperature (and consequently, any increase in concentration of surfactant) causes no additional change in surface pressure. Therefore, the profile of surface pressure versus temperature reaches a plateau above the Krafft point. The K_r value can be estimated from the intersection point of the two segments of the plot.

The surface pressure values π (dyne/cm) of saturated solutions of a surfactant at several temperatures are as follows (data read at pH 7 from Figure 3 of Pandit and Strykowski[17]).

Data for Problem 15–26

π (dyne/cm)	40	40	40	28	21.3	13.8	4.4	1.6	0.3
T (°C)	54	52	50	42	38	25	18	12	4

Plot the π values (vertical axis) against T (°C) and estimate the Krafft point of the surfactant.

Answer: $K_r = 49°$ C at pH 7

15–27. Cloud points of nonionic surfactants have been related to properties of micelles such as the critical micelle concentration (cmc) and the weight of the micelle. The effect of various concentrations of alcohol and sodium sulfate in solutions of a nonionic surfactant on the cloud point, the cmc, and the aggregation number is shown in the table.

Data for Problem 15–27

Additive	Na_2SO_4			None	Ethyl alcohol	
Concentration	0.5 N	0.3 N	0.1 N	0	5% v/v	15% v/v
Cloud point (°C)	42.7	49.7	58.0	64.0	75.9	107.0
cmc × 10^4 (wt%)	4.6	5.4	6.0	6.8	7.5	11.0
Aggregation no. (n)	301	192	142	128	106	78

Plot on a single graph both the cmc and the aggregation number, n, along the vertical axis against the cloud point (horizontal axis). Find a linear relationship between aggregation number and cloud point and between cmc and cloud point. Use any transformation of the dependent variable (the variable on the vertical axis), to the logarithm, the square root, or the reciprocal as necessary to produce straight lines. Then, compute the slope and the intercept. Comment on your results; for example, note the sign of the slope obtained, and

Data for Problem 15–25

log S	−1.208	−2.542	−2.854	−3.833	−4.0	−4.167	−4.375	−4.708
$1/T \times 10^3$(°K^{-1})	3.05	3.08	3.10	3.19	3.22	3.29	3.37	3.51

the fact that the aggregation number n is related to the size of the micelle.

15–28. The standard free energy of micellization ΔG°_m is related to the standard free energy of adsorption ΔG°_{ad} at the (air–saturated monolayer) interface through the following relationship:

$$\Delta G^\circ_{ad} = \Delta G^\circ_m - (\pi_{cmc}/\Gamma_{max}) \qquad (15-42)$$

where π_{cmc} is the surface pressure at the critical micelle concentration; and the surface excess Γ_{max} (pp. 373–375) is the maximum adsorption (in number of moles per unit area) at the air–saturated monolayer interface.

The standard free energy of micellization of n-dodecyl β-D-maltoside (DDM) in aqueous solution at 25° C is $\Delta G^\circ_m = -31.8$ kJ mole^{-1}. The surface tension of the solution at the critical micelle concentration, measured by the Du Noüy ring method, is $\gamma_{cmc} = 36.22$ mN m^{-1} at 25° C, and the surface tension of water at 25° C is 71.97 mN m^{-1} (millinewton per meter). The minimum area per molecule A_{min} at the air–saturated monolayer interface was found by Drummond et al.[2] to be 49.9 Å^2. (1 Å = 10^{-10} meter, therefore 1 Å^2 = 10^{-20} meter^2.) The maximum value of Γ, the surface excess, corresponds to the minimum area per molecule of DDM, $\Gamma_{max} = \frac{1}{N_A}\frac{1}{A_{min}}$, where N_A is Avogadro's number. Γ_{max} is expressed in mole/m^2.

Compute the standard free energy of adsorption of n-dodecyl β-D-maltoside at the air–solution interface. You will need the expressions, $\pi_{cmc} = \gamma_{water} - \gamma_{cmc}$ and $\Gamma_{max} = \frac{1}{N_A}\frac{1}{A_{min}}$.

Answer: $\Delta G^\circ_{ad} = -42.6$ kJ mole^{-1} = -4.26×10^{11} erg mole^{-1} = −10,182 cal/mole. For an explanation of the terms in equation (15–42) and its applications, see Rosen et al.[63]

15–29. Bromodiphenhydramine, an antihistaminic drug, shows surface activity and forms micelles of aggregation number $n = 11$ at 303° K. The degree of ionizatoin α and the critical micelle concentration, obtained from light-scattering experiments, are $\alpha = Q/n = 0.20$ and cmc = 9.5×10^{-4} expressed as mole fraction.[65] Compute the free energy of micellization per mole of monomeric drug. Express the results in kJ/mole. *Hint:* You will need equation (15–A8), Appendix at the end of this chapter.

Answer: $\Delta G^\circ = -31.6$ kJ/mole

15–30. Compute ΔG°, ΔH°, and ΔS° of micellization of an alkyl dimethylaminopropane sulfonate (a zwitterionic surfactant). ΔH° and ΔS° can be computed from a regression of ln(cmc) versus $1/T$. The cmc varies with temperature as follows:

Data for Problem 15–30*

cmc × 10^3 (mole fraction)	3	2.9	2.7
T (°C)	15	25	35

*Data based on B. Sesta and C. La Mesa, Colloid Polym. Sci. 267, 748, 1989.

Answer: (*Hint:* $\Delta G^\circ = RT \ln(\text{cmc}) = \Delta H^\circ - T\Delta S^\circ$.) ΔH° = 932 cal/mole, ΔS° = 14.76 e.u.; ΔG° = −3326 cal/mole, −3462 cal/mole, and −3622 cal/mole at 15°, 25°, and 35° C, respectively.

15–31. (a) Compute ΔG°_{mic} for the nonionic surfactant of formula $C_{12}H_{25}(OC_2H_4)_7OH$ in aqueous solution at 10°, 25°, and 40° C, knowing that the cmc in mole/liter ≅ mole/kg water (molality units) in this dilute solution. Therefore, the cmc values at these 3 temperatures are given as 12.1×10^{-5} m, 8.2×10^{-5} m, and 7.3×10^{-5} m, respectively.[66]

(b) Compute ΔG°_{mic}, first changing the cmc values of part (a) into mole fraction units. The molecular weight of the solvent medium (water) is 18.015 g/mole. Does the value of ΔG° depend on the units used for cmc?

(c) Compute ΔH°_{mic} and ΔS°_{mic} using mole fraction units for the cmc in equation (15–A10) (Appendix at the end of this chapter).

(d) Discuss the magnitude and sign of the thermodynamic quantities obtained for the micellization process in terms of the several kinds of interactions shown in Table 11–11, page 276.

Partial Answer: (a) Using molality units on cmc, ΔG°_{mic} (10° C) = −5.0 kcal/mole; (b) using mole fraction units on cmc, ΔG°_{mic} (10° C) = −7.3 kcal/mole and ΔG°_{mic} (40° C) = −8.4 kcal/mole; (c) over this temperature range ΔH°_{mic} = +3.2 kcal/mole; ΔS°_{mic} = +37.16 cal/(deg mole)